Modeling and Design of Compact Planar Antennas

by

Muhammad Zulfiker Alam

B. Sc. Engg., Bangladesh University of Engineering and Technology, 2000

A Thesis Submitted in Partial Fulfillment of the
Requirements for the Degree of

MASTER OF APPLIED SCIENCE

in the Department of Electrical and Computer Engineering

Supervisor: Dr. M. A. Stuchly

ABSTRACT

There is a demand for compact, low profile, and wideband antennas for modern wireless devices. The purpose of this dissertation is to develop two such antennas. A method of moments and finite difference time domain method are used for the design and analysis of the antennas. A new microstrip antenna is designed which has more than 90 % bandwidth. The operation of the antenna is explained and design equations are developed. The antenna is integrated with electromagnetic band gap structures (EBG) to examine if performance enhancement is possible. The simulation results are verified by limited measurements. A wideband loop antenna is also integrated with EBGs and significant performance improvement is achieved.

Table of Contents

Table of Figures

List of Tables

Acknowledgement

I would like to express my heartiest appreciation to my supervisor Dr. M. A. Stuchly for her continuous guidance and encouragement shown throughout this research work and the process of writing this dissertation. I cannot thank you enough for your patience and forbearance with me.

I wish to express my gratitude to K. Rambabu for his help and support during my research. I also wish to thank Dr. K. Caputa for his day-to-day help with the computers and also with the measurements. Special thanks go to Ms. Donna Shannon for her help in editing the thesis and for her help and support during the research work. My other colleagues in the lab, especially Roanna Chiu and Matt Hughes deserve special thanks for their help. Finally I wish to express my gratitude to all of my friends, especially Jahangir Hossain, Sharmina Hossain, Mahmud Hasan and my land lady Leta Richards, who made me feel that Victoria is my second home.

To My Parents

1. Introduction

1.1 Motivation

In the last few years there has been rapid advance in wireless communications. The devices are becoming smaller and they are often expected to be able to operate over several frequency bands. As a result, there is a demand for compact, low profile, and wideband antennas. With the reduction of antenna size, antenna efficiency degrades and bandwidth becomes narrower [1]. The conflicting requirements of good performance and compact size make the design of such antennas challenging.

One of the most attractive options for wireless devices is a microstrip antenna. It has many attractive features, such as low weight, compact size and low profile. However, microstrip antennas have inherent limitations, namely a narrow bandwidth and low efficiency. In recent years, considerable research has been devoted to developing wideband microstrip antennas. All the techniques reported result in antennas that are large and/or have complex structures. Since wireless devices have become very small, these wideband antennas are not well suited for such devices. Techniques for increasing antenna bandwidth without increasing antenna size deserve more research. This provides motivation for further exploration in this thesis of a modified patch antenna.

Loop antennas are another attractive option for wireless systems. They are inexpensive, simple in construction, and easy to build. Conventional loop antennas do not have sufficient bandwidth to meet present demands. Recently, a modified loop antenna with a wider bandwidth has been reported for an application on a handheld telephone [2]. While the performance is broadband, the structure of the antenna is not compatible with handsets. An investigation aimed at a modification of the antenna to place it on the handset box is undertaken in the research reported.

Electromagnetic band gap (EBG) structures have interesting features that can improve or modify performance of antennas. They can block surface wave propagation over a

frequency range. Also, they act like magnetic walls. These unique properties make them very useful in antenna applications.

One major limitation of microstrip antennas is the excitation of surface waves. This reduces antenna gain and efficiency, and also distort the radiation pattern. EBGs can reduce the surface wave propagation in their stop band, thus they enhance antenna performance.

EBGs can also be very useful for wire antennas, e.g. monopole and loop antennas. In many applications it is desirable to have radiation in one direction and block radiation in the opposite direction. The back radiation can be reduced by placing the antenna above a metal surface. However, the antenna has to be placed quarter of a wavelength above the metal, which is not acceptable in many applications. Since EBGs act as magnetic walls in the stop band, the antenna can be placed very close to the EBG surface, making the structure compact. The application of EBG structures is evaluated for both types of the antennas investigated in this thesis.

1.2 Objective and Contributions

The general objective of this thesis is to design new broadband antennas for applications in wireless communication. Due to the complex nature of the structures, it is necessary to use numerical methods for designing the antennas. The finite difference time domain method (FDTD) and method of moments (MoM) are used in the numerical modeling.

The contributions of this thesis include:

1. Broadband planar microstrip antenna: A new wideband microstrip antenna is developed. The antenna is modeled using a code based on method of moments. A parametric study is performed to optimize the antenna and the mechanism of antenna operation is investigated. The antenna is fabricated and simulation results are verified by measurements. The antenna is integrated with EBGs to further

enhance its performance. Performance of the antenna with EBGs is also evaluated experimentally.

2. Broadband loop antenna: A modified loop antenna is integrated with EBGs to improve its performance. The modeling and optimization is done using the finite difference time domain method.

1.3 Outline

Chapter 2 gives a brief overview of the present state of knowledge of broadband microstrip antennas. Various techniques for improving the bandwidth are presented and their advantages and limitations are outlined. A brief review is also provided of EBG structures and their possible applications for improving antenna performance.

Chapter 3 is on modeling methods. Two numerical methods –the method of moments (MoM) and finite difference time domain (FDTD) method have been used in this research. The principles of the two methods along with various aspects of proper modeling are presented. Two software packages based on MoM and one FDTD code have been used in this work.

Chapter 4 describes a new broadband microstrip antenna. The proposed structure is described followed by results from simulation and measurements. The mechanism of the antenna operation is explained. Performance of the antenna developed here is compared with other recently reported novel antennas. The antenna is integrated with EBGs to enhance its performance further. Those results are also presented.

Chapter 5 investigates the integration of a modified loop antenna with EBGs. The structure is briefly described followed by simulation results. Finally, Chapter 6 closes the thesis with a few concluding remarks and suggestions for possible future extension of this work.

2. Literature Review

In this chapter, a review is given of patch antennas and electromagnetic band gap structures (EBG) that are used to limit surface waves, and thus improve the antenna gain. This review is brief, as it only serves to provide the background information for placing the new designs developed in the thesis in the context of the current state of the art.

2.1 Broadband Microstrip Antennas

Microstrip antennas have many advantages, such as low profile, light weight, ease of fabrication and low cost. In addition, these antennas are mechanically rigid, which makes them less susceptible to damage than wire antennas. Microstrip antennas offer an alternative option for cellular telephone handset, as they are more compact, and potentially the amount of radiation absorbed by the user should be smaller. The major limitation of the microstrip antenna is its narrow impedance bandwidth. Typical bandwidth of a conventional microstrip antenna is 1 to 3 % (depending on the substrate) [3] compared to 15 % to 20 % bandwidth of dipole, slot or horn antennas [4]. Extensive research has been carried out during the last few decades on the possible ways of increasing bandwidth of microstrip antennas. Many different procedures have been proposed, all with varying degree of success. Furthermore, additional performance limitations may be introduced in the process of increasing the impedance bandwidth. The commonly used techniques for bandwidth enhancement are a thick substrate, external impedance matching, parasitic patches, multiple resonances and resistive loading.

Bandwidth up to 8 % for rectangular patches has been achieved by the use of a thick substrate [5]. However, for probe-fed patches, with the increase of substrate thickness, the probe inductance also increases and matching becomes difficult. To compensate the inductance, capacitance can be introduced by adding a concentric annular gap around the probe feed. This solution results in 16 % bandwidth [6]. More recently, the addition of U

shaped slot [7,8,9] and the use of an L-shaped probe [10,11] have both been shown to provide the impedance bandwidth in excess of 30 %. The U slot introduces capacitance, allowing the use of a thick substrate. It also induces a second resonance near the main resonance of the patch, thus producing a wideband frequency response. The operation of the L-probe fed patch is similar to that of the U-slot patch, with the L probe introducing the capacitance. For any feed method, surface waves are excited that lower the antenna efficiency.

An external matching circuit is an effective and simple technique for bandwidth enhancement. It does not require any modification of the antenna itself. The matching network can be a tuning stub, quarter-wave transformer section, capacitively coupled line or active device. Bandwidth up to 25 % has been achieved by this technique [12]. However, the matching circuit can also radiate and adversely affect the radiation pattern of the antenna.

Attempts have been made to enhance the impedance bandwidth by using slotted ground plane [13]. Increase in the bandwidth is not significant compared to other techniques. Furthermore, poor front to back ratio is a problem.

One of the most successful techniques for bandwidth enhancement is the use of multiple closely spaced resonances. This can be achieved by using coplanar multiple resonator element or by stacked multiple patches. Use of coplanar parasitic patches can result in bandwidth around 20 %. However, the overall size of the antenna becomes larger. Also, radiation patterns of the parasitically coupled patches are distorted within the useful impedance bandwidth. The E shaped patch reported in [14] uses multiple resonance to achieve up to 32 % bandwidth. The stacked patch configuration occupies less surface area than the coplanar patch and tight coupling is more easily achieved. An aperture-fed stacked patch can provide a very wide bandwidth [15]. This structure uses a resonant aperture, thick substrates and stacked patches. Bandwidth up to 70 % has been realized. The structure, however, is very complex and relatively thick. Therefore, fabrication of the antenna and its integration with other microwave circuitry are difficult.

Bandwidth can also be increased at the expense of efficiency by adding resistive load (loss) into the antenna system. Adding a 6 dB attenuator in series with a microstrip antenna leads to a minimum of 12 dB return loss over a broad band. The antenna gain is also reduced by 6 dB [16]. Lumped losses can be added externally using attenuators or distributed using lossy substrate materials, or added to the antenna directly by using chip resistors or other loads. This method of bandwidth enhancement is generally discouraged for microstrip antenna design, due to its relatively low radiation efficiency.

Recently, a new broadband antenna has been reported [17], which uses a single patch that has a bandwidth around 54 %. It also has relatively high gain and low cross-polarization level. The antenna, however, needs a matching network, air substrate and supporting rods for holding the patch over the air gap. As a result, it is not a very attractive solution for wireless applications. Two new antennas have been reported [18], which also have very good VSWR bandwidth and low gain. However, the antenna sizes are large compared to the wavelength.

In mobile communication systems incorporating a single linearly polarized antenna, a polarization loss is encountered when the polarization of the mobile unit varies from that of the base station. A propagating wave can be de-polarized in certain atmospheric conditions, e.g. during rainy days. Random scattering from objects and obstructions in urban environments can lead to polarization cross-coupling. Pico-cellular mobile architectures, as well as other services, may utilize dual-polarized antennas in the base station to reduce the effect of handset orientation. In addition, the dual-polarized antennas are able to transmit twice as much information as linearly polarized antennas within the same bandwidth [19].

Dual-polarized operation has been an important subject in microstrip antenna research. Many designs for achieving dual-polarized microstrip antenna are available in literature. They include single band or dual band, single feed [5] or dual feed [20,21,22] antennas. Achieving a wide bandwidth with a dual-polarized antenna is more challenging than with

linearly polarized antennas. Most broadband dual-polarized antennas utilize multiple feeds, and multiple substrates. The feed techniques for the dual-feed dual-polarized antenna include slot-coupled feeds with two crossed narrow slots, two offset narrow slots, two proximity coupled feeds, microstrip line feeds and a probe feed. A dual-polarized broadband antenna has also been developed that consists of a single patch and single probe feed [23].

Table 2.1 gives a summary comparison of patch antennas reported in literature.

Table 2.1 Characteristics of representative patch antennas

Patch type	Band	Polarization	VSWR 2:1	Gain (dB)
PIFA, meanders and rectangular [24]	Dual	Linear	7 % 6.9 %	1.0 - 2.7 1.0 - 2.1
Circular, shorting pin [5]	Single	Linear	6.8 %	3.6 (max)
Circular, arc slots [25]	Single	Linear	10.4 %	4.8 (max)
Circular, two L-shaped slots [26]	Dual	Linear	12.4 % 21.5 %	7.2 (max) 7.1 (max)
E shaped [14]	Single	Linear	32.3 %	7.5 - 8.5
Two E patches, two feeds [27]	Dual	Linear	9 % 39.4 %	9.7 - 11.2 5.4 - 6.5
Modified rectangular [23]	Single	Circular	13.9 %	4.6 (max)
Meander line probe [28]	Single	Linear	31 %	9.0 (max)
Aperture stacked [15]	Single	Linear	69 %	6.0 - 8.5
H shaped, ring slot coupling [17]	Single	Linear	54 %	3.0 - 8.0

2.2 EBG Structures for Antenna Applications

Electromagnetic band gap (EBG) structures are a class of periodic structures that exhibit transmission and reflection bands as a function of frequency. Unlike frequency selective surfaces, which also have transmission and reflection bands, EBG structures can prevent the propagation of electromagnetic waves in all directions. In addition to blocking surface waves in the stop band, for incident waves, EBGs behave as nearly perfect magnetic conductors (PMC) in the stop band and as perfect electric conductors (PEC) in the pass band. These properties make them very attractive in many microwave applications.

In the last few years, there has been extensive research on designing new EBGs and their applications in microwave devices. Many different EBG structures have been reported in literature. They can be made of dielectrics only or metallic elements embedded in dielectric. The first EBG designed for microwave applications is the mushroom structures reported in [29]. Another widely studied EBG structure is a uniplanar compact EBG (UC EBG). It consists of periodic metal patterns printed on dielectric material. This structure can be very compact and very easy to fabricate. It can be single layer [30] or multi-layer [31]. Among the numerous other different EBG structures reported, EBGs composed of multiple periodic tripods with interconnecting vias [32], air holes drilled through substrate [33] and circular slots etched in the ground plane [34] are worth noting.

Numerous applications of EBGs have been described, including those in antennas, filters, waveguides and amplifiers. In the field of antennas, EBGs have been used to enhance the performance of dipole antennas [35], spiral antennas [36], curl antennas [37], patch antennas [38], [29], bow tie antennas [39], parabolic reflectors [40] and for numerous other antenna geometries.

A very promising potential application of EBG is in telephone handsets. The presence of human head significantly changes the radiation pattern of the handset antenna and reduces its efficiency. The use of EBGs can reduce the effect of the presence of human

head. As a result, the radiation efficiency increases. The increase in the radiation efficiency extends the battery life and reduces the weight of the handset. Initial investigations of integrating EBGs with handsets [41] have shown promising results.

As indicated earlier, patch antennas are gaining popularity because of their advantages. However, one serious limitation of patch antennas is the excitation of surface waves. Surface waves reduce the antenna radiation efficiency and result in spurious radiation from the edges of the substrate. The use of EBGs can suppress surface wave over the operating frequency band of the antenna, and thus improve its performance. It has been shown that the use of EBGs can increase both antenna gain and impedance bandwidth [38].

Another example of valuable application of EBGs in antennas is high precision global positioning system (GPS). To obtain good accuracy, the antenna needs to be shielded from undesirable multi-path signals. Usually choke rings are used for this purpose. However, they are large, heavy and costly. The system size can be greatly reduced when EBGs are used as magnetic conductors. In the implementation described by Hurtado [42], the antenna weight is reduced by a factor of ten, height by a factor four and the antenna is less expensive to manufacture. It also performs much better than the horn antenna with a choke.

The transmission of incident wave through a stack of EBG layers depends on the angle of incidence. This property has been utilized to design substrate and resonant cavity antennas [43]. These antennas have highly directive radiation patterns, though they have a very narrow band.

3. Numerical Methods

A number of numerical techniques are available for antenna modeling. Each method has strengths and limitations. The choice of the method for analysis depends on a number of factors, such as the geometry of the structure to be analyzed, performance characteristics to be evaluated, and available resources. The present work utilizes two numerical methods – the method of moments (MoM) and the finite difference time domain (FDTD) method. This chapter introduces the main concepts of these techniques, and modeling features available and used of the numerical codes employed in this work.

3.1 Method of Moments

Method of moments (MoM) is the most suitable method for solving electromagnetic problem when the problem is formulated as an electric field integral equation (EFIE) or a magnetic field integral equation (MFIE). The general form of the integral equation (IE) is [44]

$$L(f) = g \tag{3.1}$$

Where L is an integral operator, g is a known source function or excitation function and f is the unknown field or response to be determined. To solve the problem, the unknown function f is expanded as a series of known basis functions (f_n) with unknown weights (α_n).

$$f = \sum_{n=1}^{N} \alpha_n f_n \tag{3.2}$$

A set of suitable testing functions (w_n) is selected and inner products are taken of both sides of equation (b) and the testing functions.

$$\sum_{n=1}^{N} \alpha_n < w_m, L(f_n) >=< w_m, g > \qquad (3.3)$$

m=1,2,....., N

This can be represented in the matrix form as

$$[A_{mn}][\alpha_n] = [g_m] \qquad (3.4)$$

where $A_{mn} =< w_n, L(f_m) >$ and $g_m =< w_m, f >$

The solution of equation (d) can be found by matrix inversion.

$$[\alpha_n] = [A_{mn}]^{-1}[g_m] \qquad (3.5)$$

The choice of the integral equation (IE) depends on the problem to be solved. For example, Hallen and Pocklington [44] have developed IEs that are well suited for modeling thin wires. Araki.et al [45] have developed equations suitable for open microstrip structures

There are several approaches for IE formulation. [46, 47]. The most straight forward is the EFIE or MFIE formulation. The Green's functions in these formulations involve Sommerfeld integrals, which have no analytical solution. This approach is sometime taken for laterally open structures where homogeneous dielectric layers are assumed to extend to infinity.

A problem with this formulation is the strong singularity of the Green's function, which makes its direct evaluation impossible. The strong singularity can be avoided by making use of vector and scalar potentials in the problem formulation. This approach is known as mixed potential integral equation (MPIE) formulation. It is widely used in MoM code implementations. A variation of MPIE, the iterative mixed potential integral equation (IMPIE) method combines the advantage of MPIE with the speed of fast Fourier transform (FFT) algorithm.

Strong singularities can also be avoided by adopting the spectral domain approach. This approach is suitable for closed box cases, where the structure is enclosed by metallic walls. By taking two-dimensional Fourier transform in the transverse direction, a set of transverse modes of fields and currents can be obtained. The spectral components of the Green's function can be found and then the inverse Fourier transform can be taken to revert to the space domain. The rest of the analysis can be performed in the space domain. It is also possible to formulate the integral equation in the spectral domain and then to apply the method of moments in the spectral domain. At the end of the solution, inverse Fourier transform gives the spatial current distribution. Both approaches are used in practice.

A limitation of the MoM solution technique is the need for inverting a large, dense matrix. The matrix size becomes too large when the structure is inhomogeneous and irregular in shape and material properties. The MoM techniques are also not well suited for analyzing the interior of conductive enclosures or thin plates with wire attachments on both sides [48]. Nevertheless, MoM techniques do an excellent job of analyzing a wide variety of important three-dimensional electromagnetic radiation problems. They are very suitable for multilayered circuit board applications, planar structures such as microstrip antennas and electromagnetic scattering problems.

3.2 Finite Difference Time-Domain Method

The finite difference time domain (FDTD) is a very popular technique based on the differential form of Maxwell's equations. The FDTD can be readily applied to complex geometries consisting of inhomogeneous dielectrics and metal objects. The method, introduced in 1963 by Yee [49] is a direct solution of two Maxwell's equations:

$$\nabla \times \overline{H} = \overline{J} + \frac{\partial \overline{D}}{\partial t} \qquad (3.6)$$

$$\nabla \times \overline{E} = \overline{M} - \frac{\partial \overline{B}}{\partial t} \qquad (3.7)$$

where $\overline{E}$ and $\overline{H}$ are the electric and magnetic field strengths, $\overline{J}$ and $\overline{M}$ are the electric and magnetic current densities, and $\overline{D}$ are the $\overline{B}$ electric and magnetic flux densities. All of the field quantities are functions of space and time. The FDTD method solves these two equations by discretizing both space and time using a finite difference approximation. Among different finite difference approximations, the central difference approximation is the most popular because of its accuracy. For a function f (x,y,z,t), the central difference approximation is given by the following relation

$$\frac{\partial f(x,y,z,t)}{\partial x} \approx \frac{f(x+\frac{\Delta x}{2},y,z,t) - f(x-\frac{\Delta x}{2},y,z,t)}{\Delta x} \qquad (3.8)$$

where Δx is an increment in the x direction. The application of the central difference approximation to (A) and (B) produces a set of six scalar equations [49]. Thus, unlike in some other numerical methods, the solution of the field quantities does not depend on inversion of large matrices, which is a great advantage of the FDTD method. However, $\overline{E}$ and $\overline{H}$ have to be evaluated at all nodes in the computational space. The general strategy for FDTD solution was outlined by Yee [49]. As shown in Figure 3.1, $\overline{E}$ and $\overline{H}$ are evaluated at different positions of the grid. They are also evaluated at alternate time steps.

Care must be taken to ensure numerical stability in an FDTD analysis. The computed result may spuriously increase without limit. To ensure numerical stability, the time increment Δt has a specific bound relative to the space increments Δx, Δy and Δz. This limit, known as Courant limit, is investigated in [50]. The FDTD algorithm is at first divided into separate time and space eigenvalue problems. The existence of complete three dimensional spatial Fourier mode spectra for the E and H fields are assumed in the grid. The complete spectrum of eigenvalues for these spatial modes due to the FDTD algorithm is determined. By requiring that the complete spectrum of spatial eigenvalues

be contained within the stable range, numerical stability is ensured. Following the procedure, the condition for the time step is achieved:

$$\Delta t \leq S\sqrt{\mu\varepsilon}\left[\frac{1}{\Delta x^2}+\frac{1}{\Delta y^2}+\frac{1}{\Delta z^2}\right] \tag{3.9}$$

where μ and ε are the permeability and permittivity of the medium, respectively, and $S \leq 1$ is the stability coefficient. For sufficient accuracy of the results, spatial increments in the Yee grid (Δx, Δy, Δz) must be sufficiently small (typically λ/10 - λ/20) compared to the shortest wavelength, and a sufficient number of time steps must be chosen [51]. Even smaller grids have to be used in regions where fields change rapidly. Proper attention has to be paid also to the boundary conditions and the accurate modeling of the metals, dielectric materials and the source excitation.

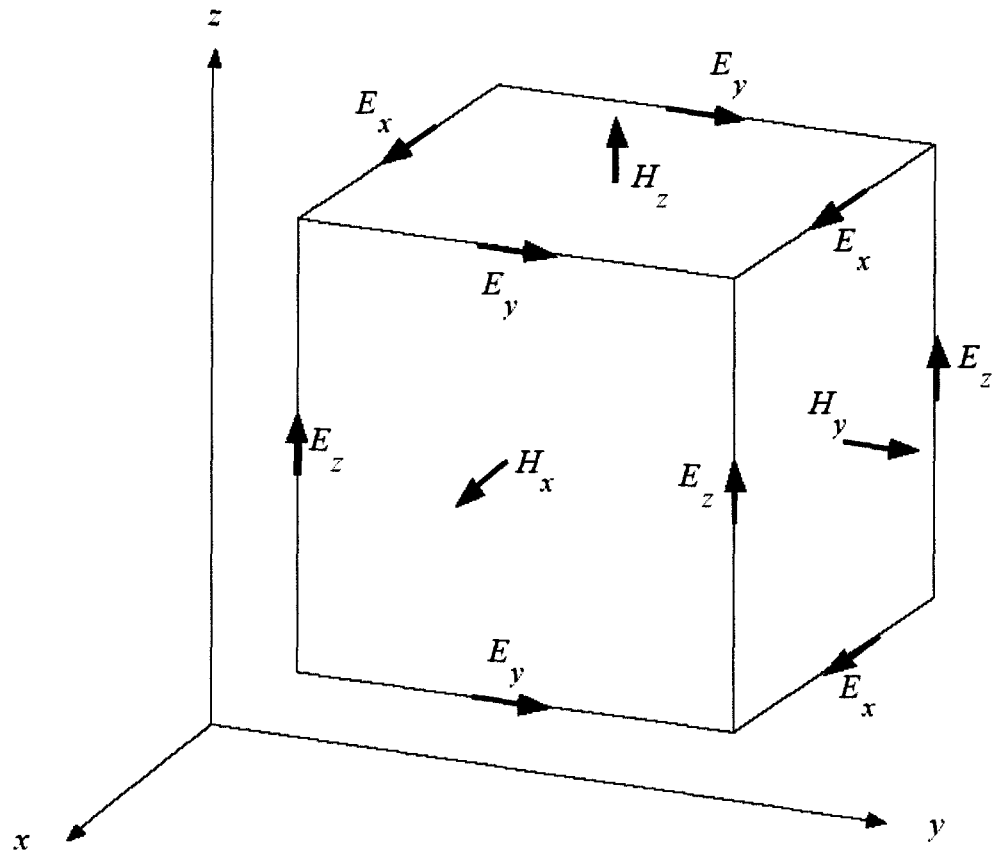

Figure 3. 1 Yee cell in FDTD method

The FDTD formulation requires absorbing boundary condition (ABC) to simulate the effect of an unbounded region. Proper modeling of ABC is a very important issue in FDTD. Many different ABCs have been proposed, each with its relative advantages and limitations. The most general and widely used ABC is the perfectly matched layer [PML] introduced by Berenger [52]. The PML can provide a reflection smaller than –60 dB to –110 dB for an arbitrary angle of incidence even when the boundary is placed only 5 cells from the surface of the scatterer.

Another important issue in the FDTD formulation is modeling of the excitation source. Application of update equations makes sense only if either initial conditions are given or if an energy source is applied. Since nontrivial initial conditions cannot usually be easily specified, the system is most often excited by a source. There are many source models

available. The simplest one is the so-called hard source: field components at some locations are given pre-defined values in time domain, while the other field values are updated in the usual manner. The problem of the hard source is that any reflected wave returning back to the source will be perfectly re-reflected. To make the source transparent to the reflected waves, the system can be excited using an additive source term [53]. Such a source is called a soft source. For probe-fed patch antennas, an important excitation case is the modeling of a coupling probe formed from an extension of the inner conductor of a coaxial cable. There are several options for modeling this, of which two common are modeling the source as an equivalent delta-gap [54], and modeling the coaxial cable as a separate one dimensional structure and connecting it to the FDTD volume using a special technique [55].

Special care has to be exercised when the shape of the object does not conform to the FDTD grid. For example, problem arises when a metal sheet is modeled whose thickness is less than the size of a cell. The conventional FDTD algorithm either ignores the metal sheet or it assumes the metal to occupy the entire volume of the cell. Either assumption results in error, which may be considerable. A number of ways have been proposed to solve the problem. The most obvious way is to use a finer grid size over the whole computational volume. However, it significantly increases the computational burden and memory requirement. Many other alternatives have been suggested. These include non-uniform gridding, subcell gridding, subcell modeling, nonorthogonal and curvilinear grids, subcell modeling, nonuniform orthogonal grids and extrapolation techniques [56]. Nonuniform grids are gradually denser near the small features. In subcell gridding method, a fine grid is used around the small features and a regular coarse grid is used in the remaining region. Subcell modeling is often used when it is impractical to decrease the mesh size to the fine features of the object, even if subcell or nonuniform meshing is used. This is commonly used to model thin sheets, slots, wires and metal sheet edges. In subcell modeling, rather than modifying the grid, the update equations are modified near the fine structure. The modified update equations are usually based on integral form of Maxwell's equations, which takes into account the field behavior in the region of interest. Another approach is to use non-orthogonal grids similar to those used in the finite

element method. This approach, however, is not robust and is not suitable for handling different structures with a minimum amount of preprocessing, which is one of the principal attractive features of FDTD. The modeling accuracy can be greatly improved by using a nonuniform but orthogonal grid. It offers a good compromise between the uniform and nonorthogonal discretization. This technique is widely used in FDTD implementations.

3.3 Selection and Overview of Software Packages Used

There is no numerical technique that works better than any other technique for all antenna problems. Each method has its advantages and limitations. One method may be ideally suited for a particular problem and may not be very well suited for other problems. Before selecting a numerical method for a specific problem, it is necessary to consider the relative merits and limitations of different methods.

Method of moments (MoM) is very suitable for planar structures. It works well for structures with thin conductors and homogeneous, layered dielectrics. For such structures, MoM discretizes the structure only in two dimensions and concentrates most of the numerical effort to the currents flowing through parallel metallic conductors. As a result the amount of computation is greatly reduced. However, MoM needs the inversion of a dense matrix, which is large for many practical antenna designs. When either the metal is thick or dielectric material is inhomogeneous, the amount of computation is significantly increased. Therefore, MoM is not very well suited for complex structures.

The finite element method (FEM) is the method of choice for structures of complex and irregular shape in three dimensions. The greatest advantage of FEM is its ability to analyze a wide variety of problems. It can easily model structures with complex geometries. Even relatively small details in a large structure can be modeled. However, unlike MoM the whole volume has to be discretized. As a result, FEM solution needs the inversion of a large, sparse matrix.

The FDTD is a very powerful time domain technique. It does not require matrix inversion and needs less memory than FEM and MoM. The frequency response over a broadband can be found by the Fourier transform of the time domain data from a single FDTD simulation. FDTD can model nonlinear materials and devices very easily. FDTD code is naturally compatible with parallel processing. All these features make the FDTD very attractive for accurate analysis of large, complex structures when proper computational facility is available.

As mentioned earlier, the selection of numerical modeling method depends on the problem to be solved and the availability of software and computer resources. For planar structures, MoM is the method of choice. Thus, initially IE3D (product of Zeland Corporation) was selected for modeling the microstrip antenna in this research work. On the other hand, for the modeling of the loop antenna on a telephone handset, it was anticipated that an FDTD or FEM code would be required because of the 3 dimensional geometry is not likely to be compatible with the Green's function used in MoM formulation.

Initial modeling of the microstrip antenna was performed with IE3D. However, as described in section 4.1, this software did not perform satisfactorily for the antenna developed in this research. Subsequently, Ansoft Designer (product of Ansoft Corporation) was selected. For modeling of the loop antenna, an FDTD code developed in University of Victoria was used.

Ansoft Designer is a method of moments based software package developed by Ansoft Corporation. It is an improved version of the popular package Ensemble developed by the same company. The software is capable of handling a variety of problems and can be used for design and analysis of linear and nonlinear circuits. [57]

To generate a solution of electromagnetic fields for a planar circuit, Ansoft Designer employs the mixed-potential integral equation (MPIE) method. The surface of the

geometric model is automatically divided into triangles and rectangles. A volume mesh is not generated inside the model because at high frequencies, since the skin depth is negligibly small, a surface mesh is sufficient. Once the surface mesh has been generated, the following MPIE is applied to it:

$$\hat{n} \times (-j\omega A - \nabla\phi) = \hat{n} \times Z_s J \qquad (3.10)$$

Here $\hat{n}$ is a unit vector perpendicular to the face of the triangles, ω is the angular frequency, A is the magnetic vector potential, ϕ is the electric potential, Z_s is the surface impedance, and J is the current density. The method of moments (MoM) is applied to the MPIE to solve for J, the current distribution on the surface mesh. Then the S-parameters and the radiated fields are calculated from J.

There is a trade-off between the size of the mesh, the desired level of accuracy and the amount of available computing resources. The accuracy of the solution depends on the size of the basis elements. Solutions based on fine meshes are more accurate than solutions based on coarse meshes. To generate a precise description of the current, each element of the mesh must occupy a region that is small enough for the current to be adequately interpolated from the normal values. However, meshes with a large number of elements require a significant amount of computing power and memory. Therefore, it is desirable to use a mesh that is fine enough to obtain an accurate current solution but not so fine that it exhausts the available computer memory and processing power. Ansoft Designer supports two types of solution set up- fixed meshing and adaptive meshing.

In adaptive meshing scheme, to produce an optimal mesh, Ansoft Designer uses an adaptive, or iterative process in which the mesh is automatically refined in critical regions. First, a solution based on a coarse initial mesh is generated. Then, the mesh in critical areas is refined and a new solution is generated. When the current and charge distributions on the structure converge to within the desired precision, the process is terminated. The algorithm for adaptive analysis is shown in Figure 3.2.

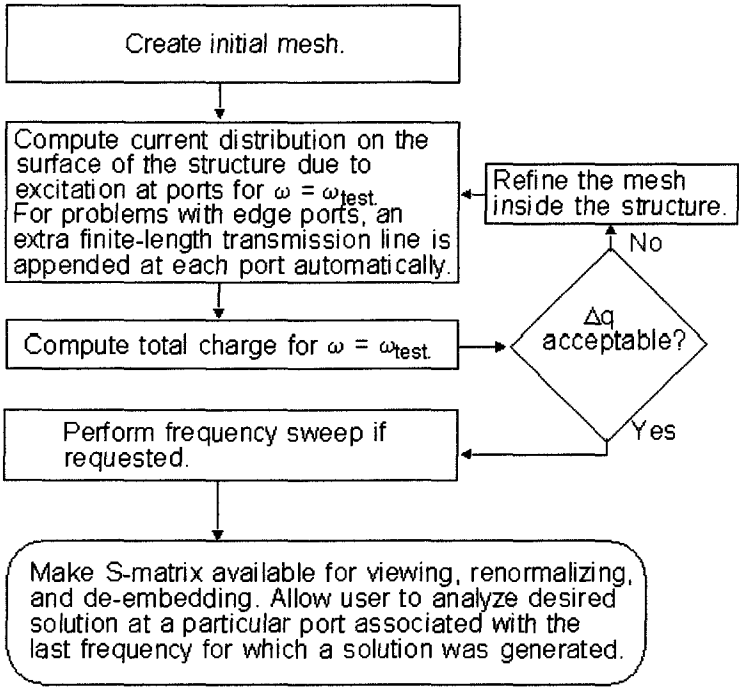

Figure 3. 2 Flowchart of solution using adaptive meshing scheme

Alternatively, a fixed dense mesh can also be used by choosing the fixed frequency meshing option and specifying a frequency near the high end of the range of interest. The mesh generated using this option is a uniform mesh. The advantage of the fixed frequency mesh over the adaptive mesh is that no extra simulations are needed to generate the mesh before the frequency sweep can be done. When fixed mesh solution setup is chosen, Ansoft Designer has the option of adding narrow rectangles along the edges of the model. These rectangles efficiently capture electromagnetic effects close to the model edges, resulting in faster solution times and higher accuracy. When Ansoft Designer defines the fixed mesh, it determines the length of the rectangles (the longer edges, which lie parallel to the model edge) by making them smaller than a fraction of the wavelength at the specified frequency. The widths of the rectangles are defined by specifying the ratio of the rectangles length to the width (edge mesh length ratio). The ratio value should be between 0.02 and 0.2 to prevent extremely narrow rectangles and extremely wide triangles.

An FDTD code "Totem" was developed at University of Victoria. It is a very poweful software package, capable of handling a wide variety of structures and its accuracy has been tested over years for many problems.

Totem supports several boundary conditions, namely PML, GPML, Mur's ABC, and electric and magnetic wall. It also supports periodic walls for normal incidence of the wave. The latter feature is important for modeling of periodic structures such as EBGs.

Sub-gridding and graded meshes are supported by this package.The excitation sources include a single impulse, gate pulse in time, gaussian impulse, ramp functions, and others. Special features also include conformal modeling of metallic volumes, thin metal sheets and dielectric averaging.

4. Broadband Microstrip Antenna

4.1 Introduction

In this chapter a novel microstrip antenna is described. Definitions of the basic antenna parameters are outlined in Appendix A. The novel antenna provides a relatively wide impedance bandwidth. The antenna is an extension of earlier works reported elsewhere [23]. The proposed antenna is a two-layer structure fed by a single element. Compared to other broadband microstrip antennas, it is very compact and has a very wide bandwidth. The antenna is first analyzed using method of moments and design equations are developed. A prototype is built and measurements are carried out to confirm the simulation results. The antenna is then integrated with EBGs for enhancing its performance further.

To model this antenna MoM code IE3D was selected and prior to its use, it was tested on other similar antennas described in literature. Results of these investigations are summarized in Appendix B. However, despite satisfactory results obtained for these antennas, the code failed to perform satisfactorily in the case of the new antenna (see Figure 4.3). Subsequently, another MoM code Ansoft Designer, is used after its performance has been compared with that of codes based on other methods and measurements.

4.2 Antenna Design and Analysis

The structure of the proposed antenna is shown in Figure 4.1. Three square patches are overlapped along their diagonals. The dimensions of the squares are (W_1 x W_1), (W_2xW_2) and (W_3xW_3), respectively. Dimensions S_1 and S_3 are the overlap dimensions. The probe position is adjusted to give a resistance close to 50 Ω over the range of operation. The inductance of the patch is large due to the coaxial feed. A capacitive element is used to

compensate this inductance. A square metal pad is attached to the inner conductor of the coaxial line and placed below the antenna with a gap between them.

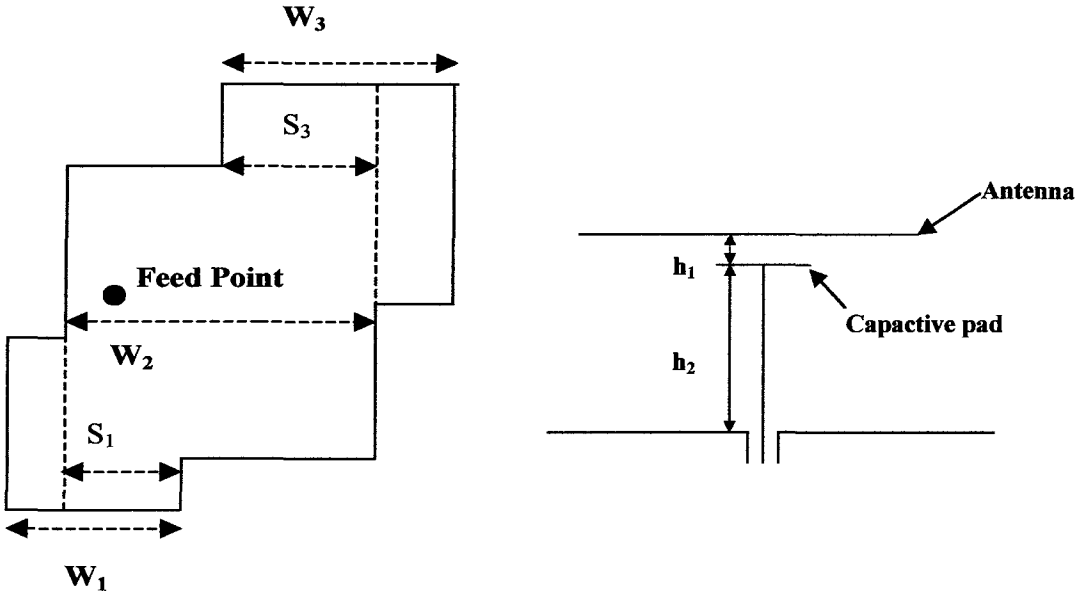

Figure 4. 1 Geometry of the proposed antenna

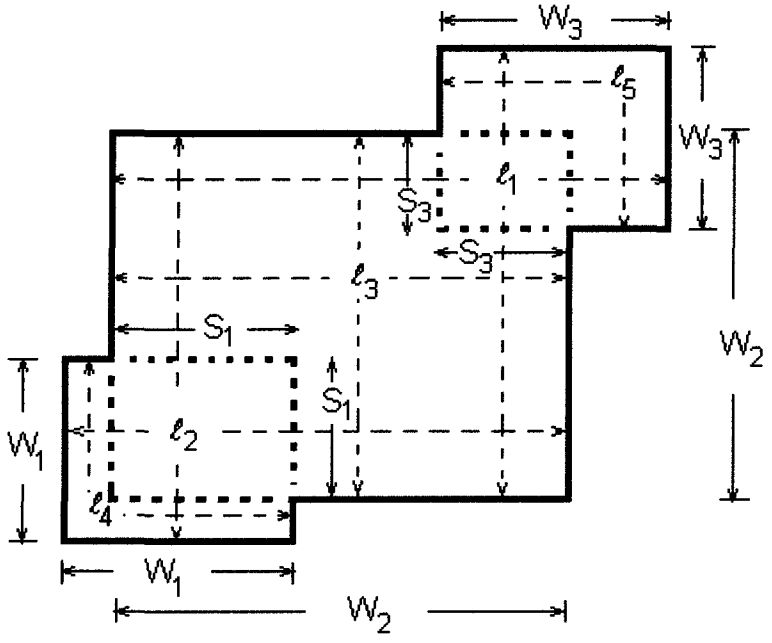

Figure 4. 2 Resonating lengths of the proposed antenna .

Figure 4.2 shows the different resonating lengths of the antenna. The structure has six different resonant lengths. Approximate expressions for the resonant lengths are [58].

$$l_1 = W_2 + (W_3 - S_3) + 2\Delta l_1 \quad (4.1)$$

$$l_2 = W_2 + (W_1 - S_1) + 2\Delta l_2 \quad (4.2)$$

$$l_3 = W_2 + 2\Delta l_3 \quad (4.3)$$

$$l_4 = 2W_1 - (W_1 - S_1) + 2\Delta l_4 \quad (4.4)$$

$$l_5 = 2W_3 - (W_3 - S_3) + 2\Delta l_5 \quad (4.5)$$

$$l_6 = \sqrt{2}W_2 + 2\Delta l_6 \quad (4.6)$$

The $\Delta l_1, \Delta l_2, \Delta l_3, \Delta l_4, \Delta l_5$and Δl_6 are the equivalent widths accounting for the fringing field [59], corresponding to line widths l_1, l_2, l_3, W_1, W_3 and the shorter diagonal respectively.

The antenna was first optimized using MoM-based package IE3D. A prototype was built and measurements were carried out using network analyzer HP 8720 C. The results were significantly different from those obtained from IE3D. Therefore, it was necessary to simulate the structure using other codes. The simulations were also performed using FEM code HFSS, FDTD code Totem and MoM code Ansoft Designer. Figure 4.3 shows the comparison between the measurements and simulation results. All the software packages except IE3D show close agreement with measurements. MoM code Ansoft Designer can handle planar structures very efficiently. It also requires less time and computer resources. Therefore, all the remaining investigations of this antenna are done using Ansoft Designer.

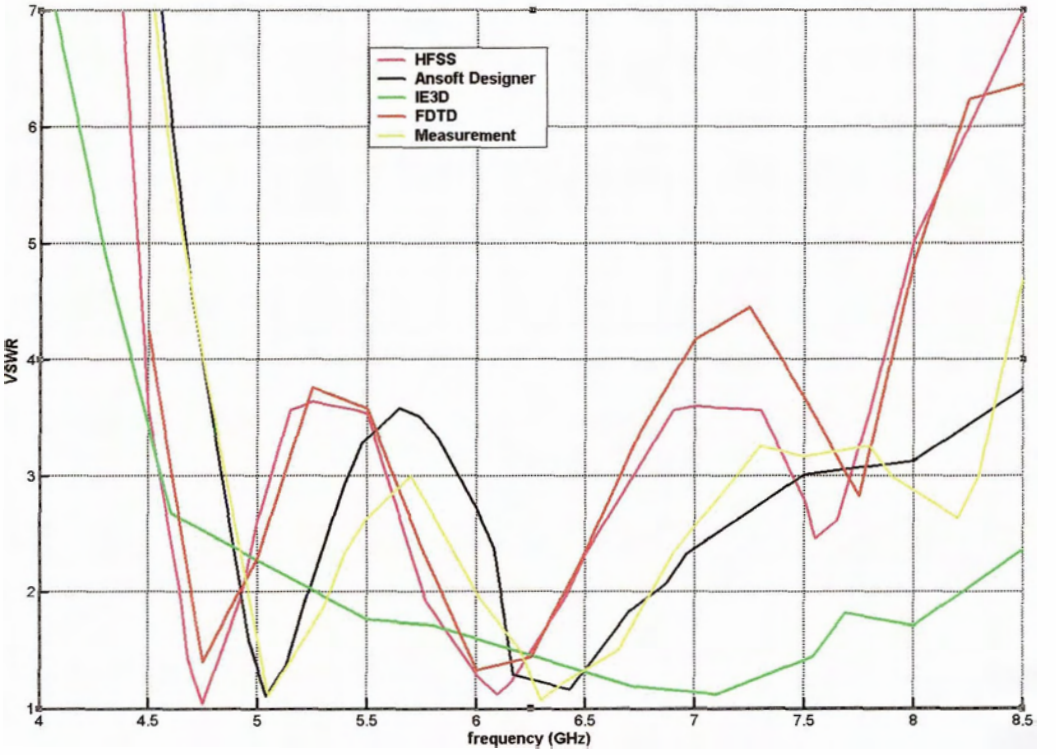

Figure 4. 3: Comparison of measurements and simulation results from different software packages

A patch antenna is designed on a RT Duroid 5870 substrate with a relative permittivity of $\varepsilon_r = 2.35$. The dimensions of the antenna are W_1=8 mm, W_2=13.5 mm, W_3=9.5 mm, h_1=0.8 mm, h_2=3.175 mm. A square metal sheet of size 4 ×4 mm is attached to the inner conductor of the coaxial line and placed below the patch with a gap of 0.8 mm to provide the compensating capacitance. After the preliminary selection of the patch dimensions based on the operating frequency, commercial software, Ansoft Designer, is used to simulate the structure. Based on the simulation results, the dimensions are modified and the probe position is optimized to get satisfactory performance over the intended frequency range of operation.

Figure 4.4 shows the variation of input resistance and reactance with frequency.

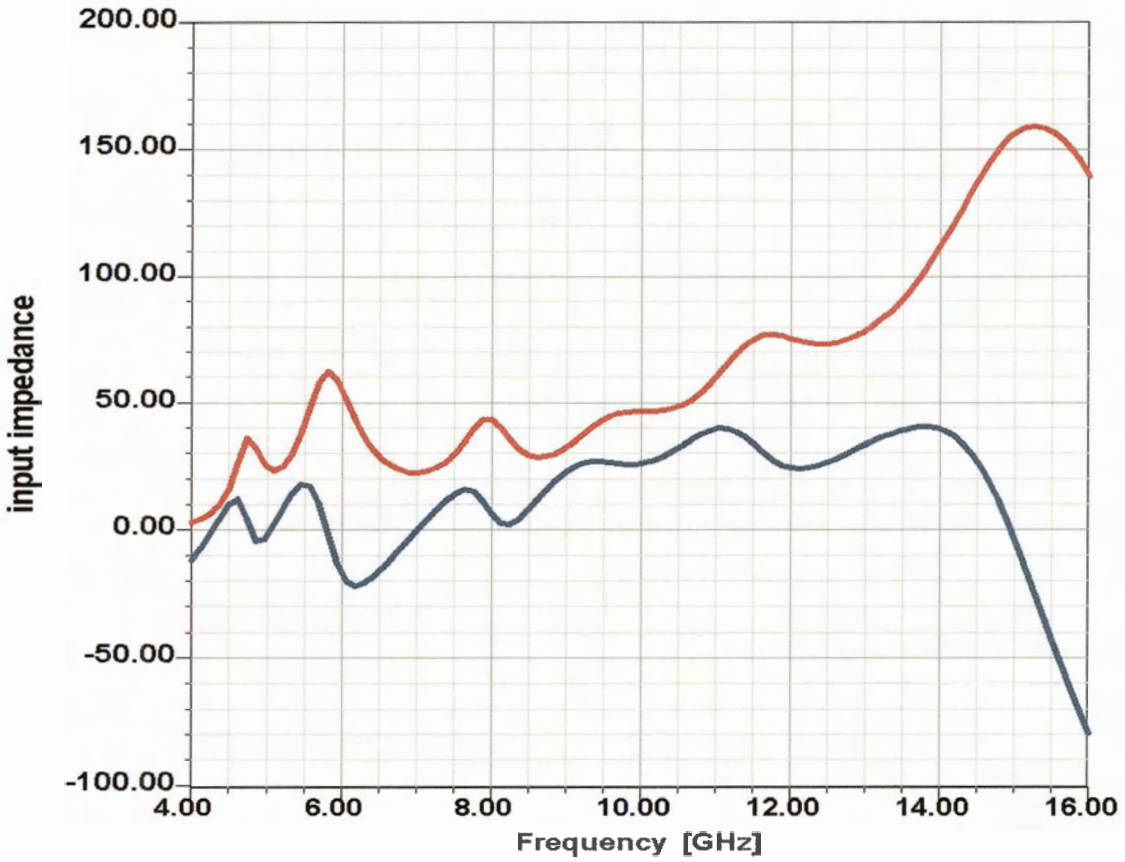

Figure 4. 4 Variation of input resistance (red curve) and input reactance (green curve) with frequency

From Figure 4.4, it is seen that the antenna shows 12 resonances. The lower six are the fundamental modes. The next six resonances are harmonics of the lower ones. Table 4.1 compares the resonance frequencies obtained from simulation with those from the formulas (equations (4.1) to (4.7)).

Table 4. 1 Comparison of resonance frequencies obtained from simulation with those obtained from the approximate theory

Resonant dimensions (mm)	Resonant frequencies (GHz)		
	Equations	Simulation	Difference (%)
Longer diagonal = $[13.5+2.5+1]^{0.5}$	3.68		
Shorter diagonal =19.09	4.44	4.18	5.7
l_1=16	4.93	4.74	3.9
l_2=14.5	5.41	4.9	8.3
l_3=13.5	5.80	5.79	0.1
l_5=17.5	6.97	7.12	2.2
l_4=14	8.03	7.85	2.2
Harmonic of shorter diagonal	8.88	8.50	4.2
Harmonic of l_1	9.86	9.77	0.9
Harmonic of l_2	10.82	10.45	3.4
Harmonic of l_3	11.59	11.61	0.2
Harmonic of l_5	13.94	12.76	8.5
Harmonic of l_4	16.06	15.33	4.6

The presence of so many resonances suggests the possibility of a very wide bandwidth. After further parametric study and optimization, a broadband performance was achieved as shown in Figure 4.5. The antenna has an impedance bandwidth with VSWR < 2.2 of 95.45 % (4.6 - 13.0 GHz).

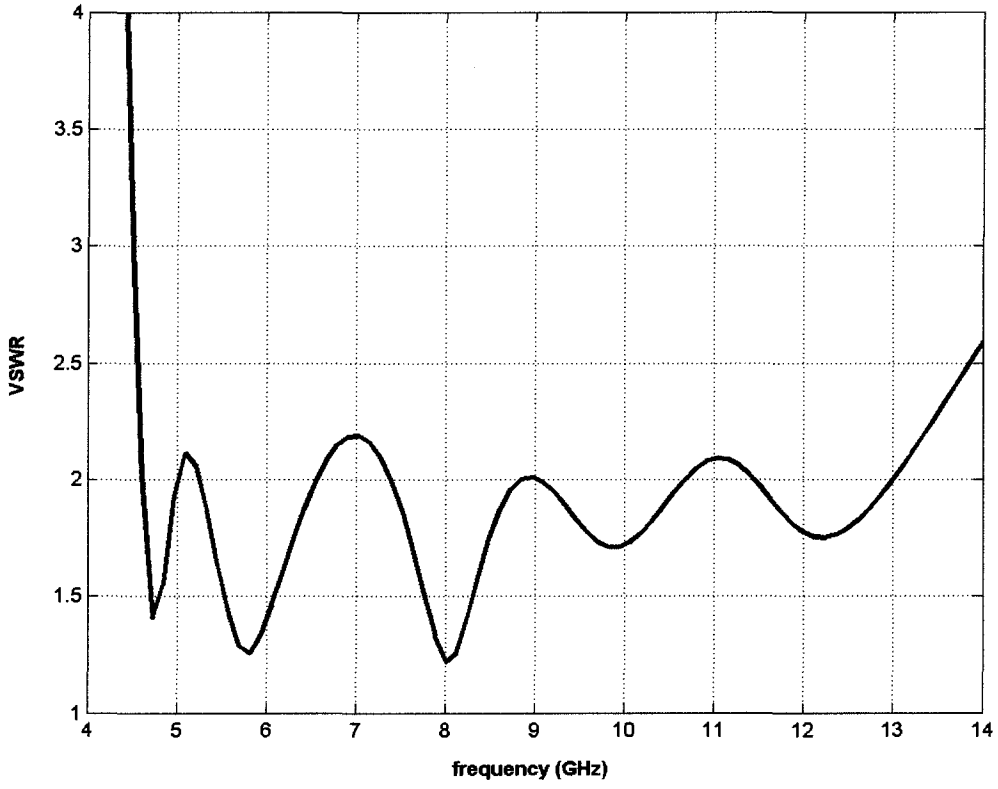

Figure 4. 5 VSWR of the antenna (VSWR ≤ 2.2 for 4.6 – 13.01 GHz)

Gain plots of the antenna in two different directions (θ=0°, ϕ=0° and θ=30°, ϕ=45°) are shown in Figure 4.6. The antenna has relatively good gain over the entire impedance band.

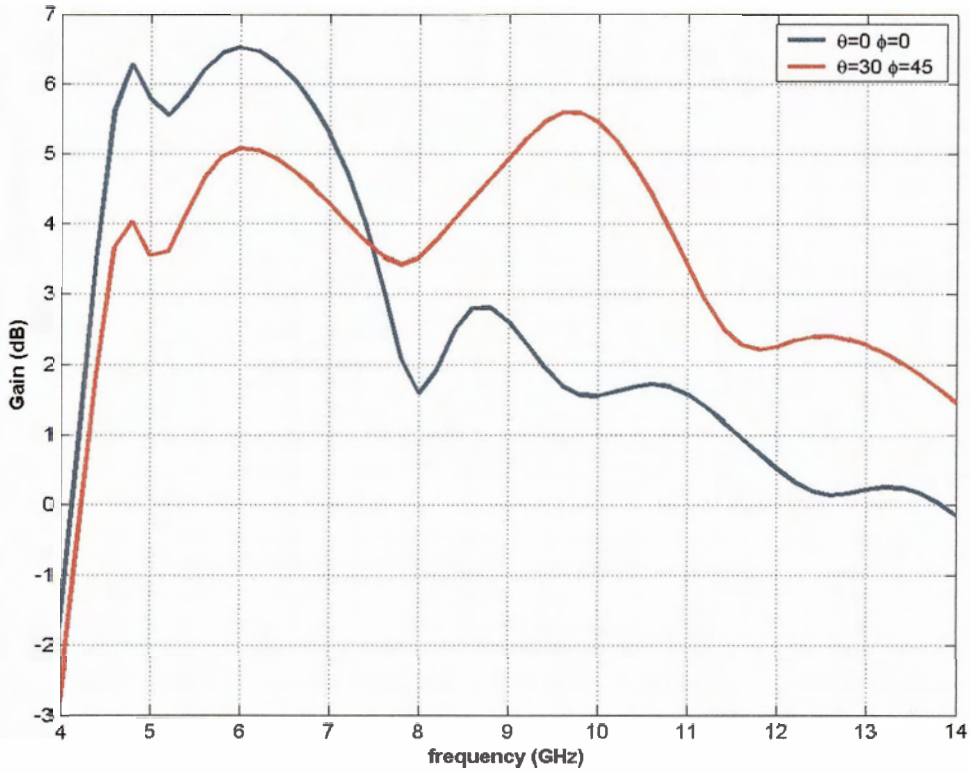

Figure 4. 6 Gain of the antenna in two different planes

The radiation patterns in two principal planes of the antenna at different resonance frequencies are shown in Figure 4.7. Radiation patterns in 3D at different resonant frequencies are shown in Figure 4.8.

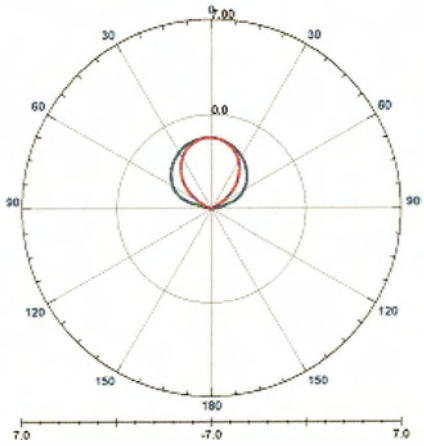

(a) 4.18 GHz

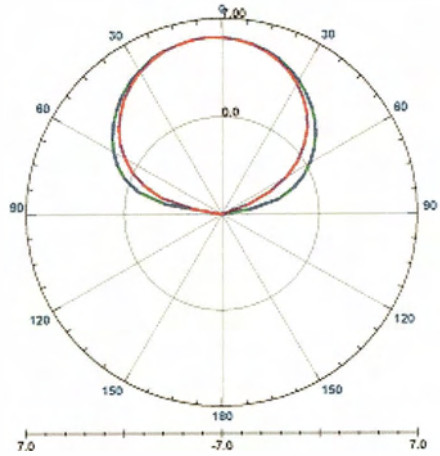

(b) 4.74 GHz

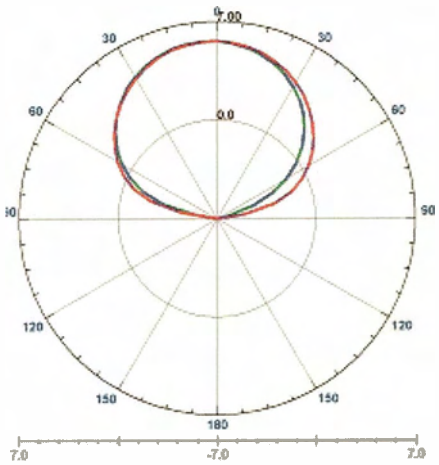

(c) 4.9 GHz

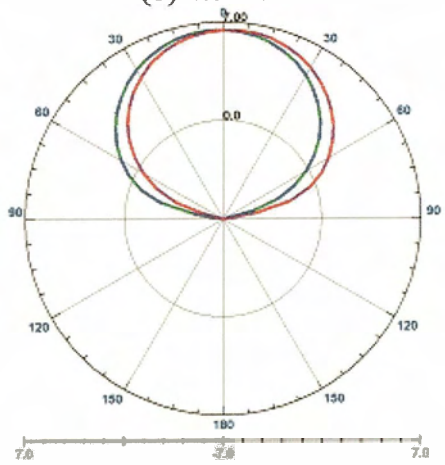

(d) 5.79 GHz

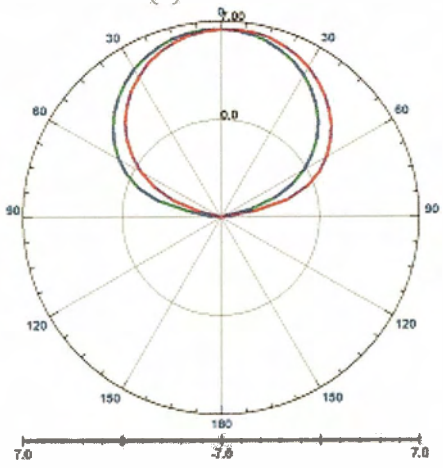

(e) 7.12 GHz

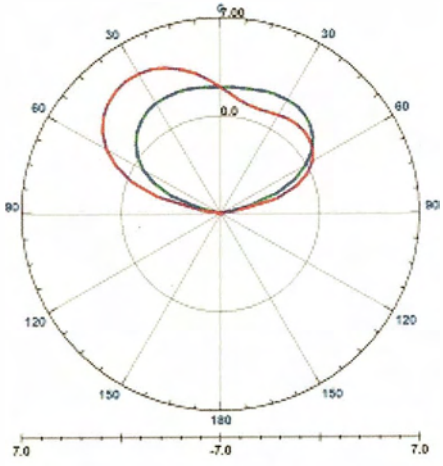

(f) 7.85 GHz

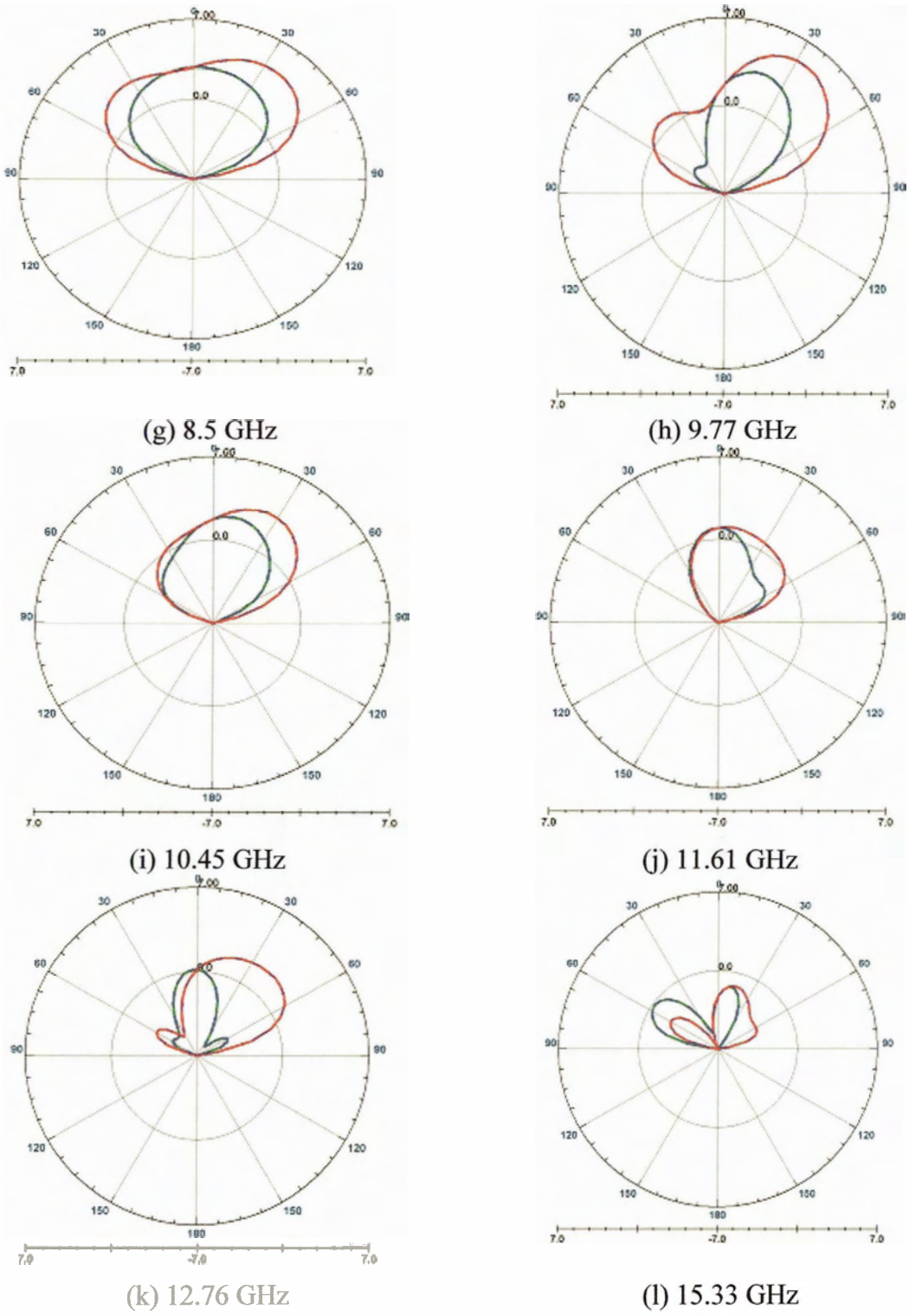

Figure 4. 7 Radiation patterns at different resonance frequencies; red line for ϕ=0° plane and green line for ϕ=90° plane. Gain scale in dB.

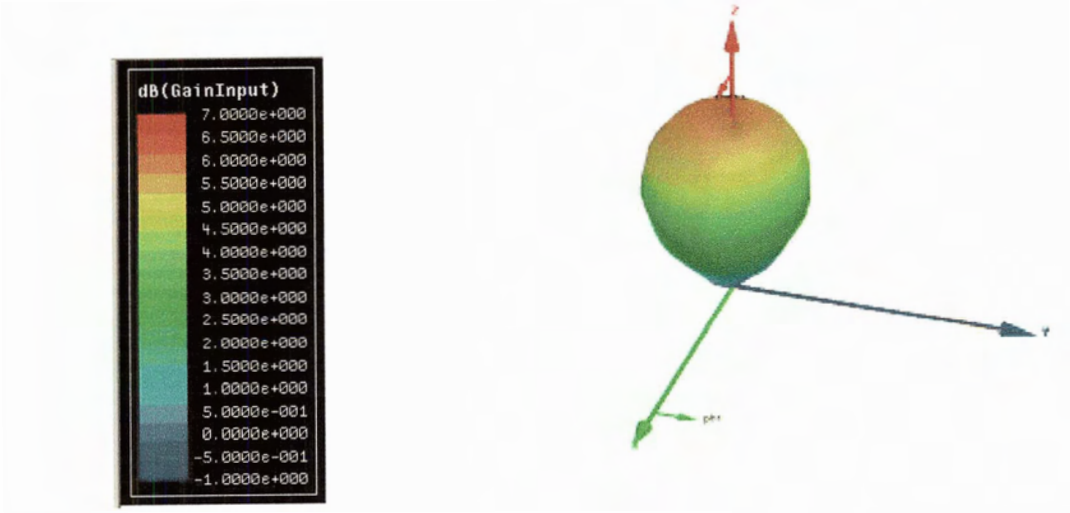

(a) 4.74 GHz

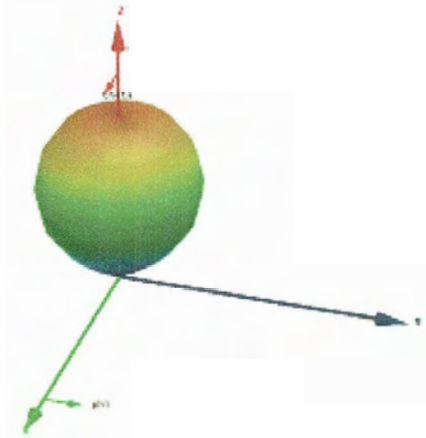

(b) 4.9 GHz

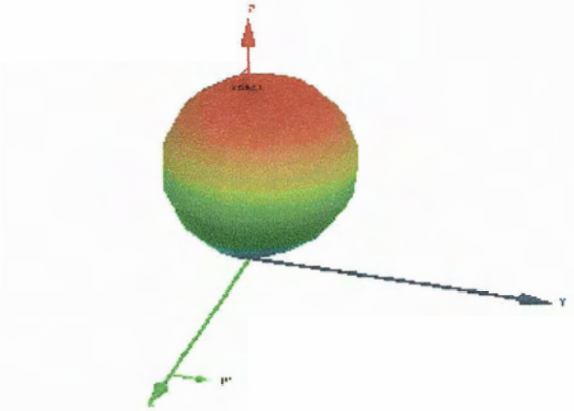

(c) 5.79 GHz

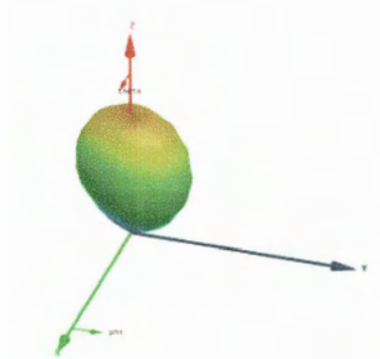

(d) 7.12 GHz

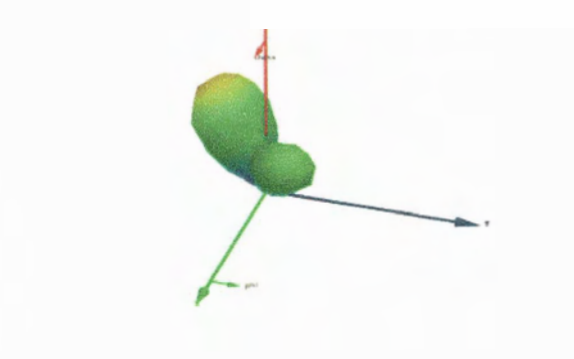

(e) 7.85 GHz

(f) 8.5 GHz (g) 9.77 GHz

(h) 10.45 GHz (i) 11.61 GHz

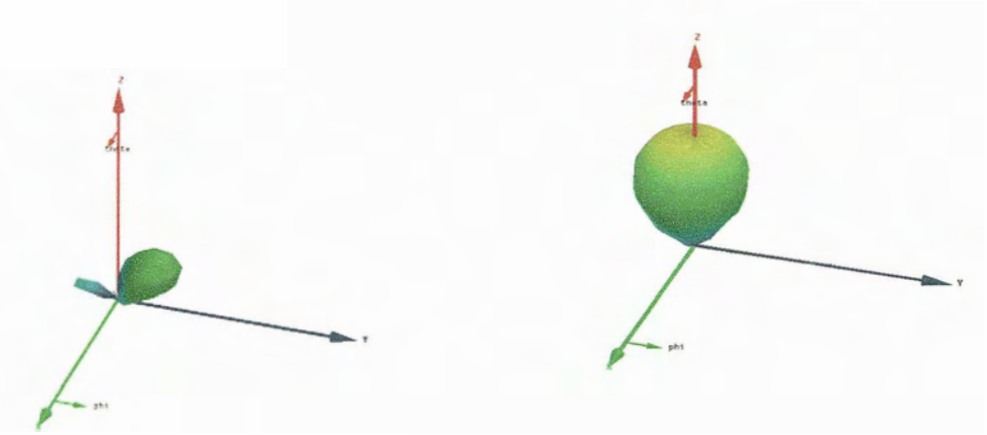

(j) 12.76 GHz (k) 15.33 GHz

Figure 4. 8: Radiation patterns at different resonant frequencies (in dB) in same scale as shown in Figure 4.8 (a)

From the radiation patterns and gain plots, it is apparent that the shape of the beam and direction of maximum gain vary with frequency. Furthermore, the beam is tilted from bore sight at higher frequencies. The effect is most pronounced near 7.85 GHz. At 7.85 GHz, the gain at bore sight falls below 2 dB, although the gain in other direction is much greater.

To better understand the antenna operation, the field distributions under the patch at different resonant frequencies are plotted in Figure 4.9. The field distribution under the patch is very complex and it is very difficult to identify the resonant lengths from these plots. However, it can be observed that at each resonant frequency, the antenna has radiating sides in perpendicular directions. Thus, the antenna provides dual polarization. Also, the field strengths at different sides of the patches are not equal. Therefore, the beam is tilted toward the side where the field is stronger. Maximum gain is at bore sight for lower frequencies, but at higher frequencies the maximum gain is in other direction. To examine the reason behind this, the current distributions at two frequencies (5.79 GHz and 7.85 GHz) are shown in Figure 4.10. In patch antennas, each of the two opposite sides acts as a radiating slot and two opposite sides of the antenna form an array. The directions of current flow at two opposite sides of the patch are in the same direction at 5.8 GHz, but in opposite direction at 7.85 GHz. This indicates that the phase relations between the fields at these two frequencies are opposite to each other. As a result, while the radiations from two opposite edges add in bore sight at 5.8 GHz to form a maximum there, they cancel each other at 7.85 GHz and form a minimum in the same direction.

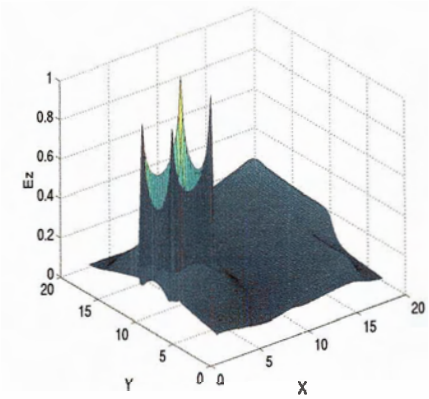

(a) 4.18 GHz

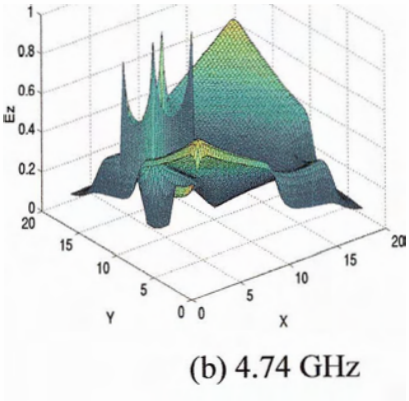

(b) 4.74 GHz

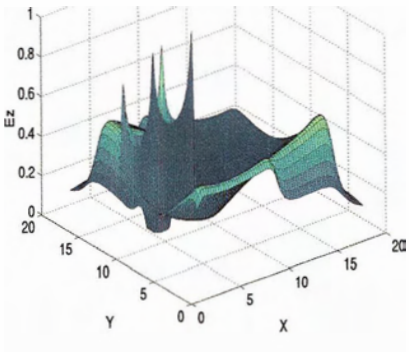

(c) 4.9 GHz

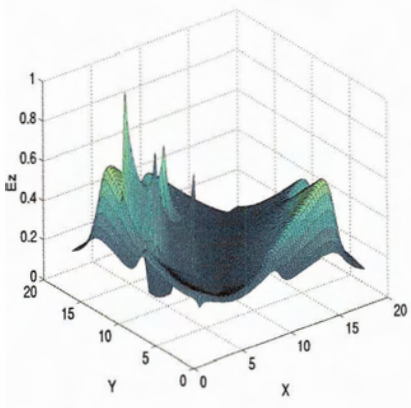

(d) 5.79 GHz

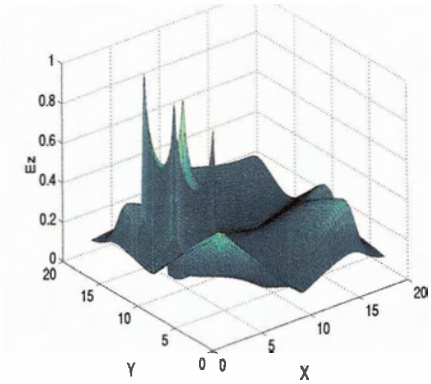

(e) 7.12 GHz

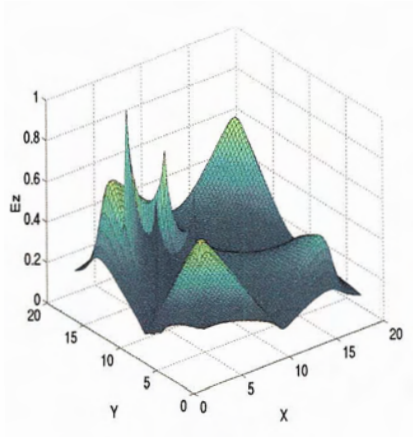

(f) 7.85 GHz

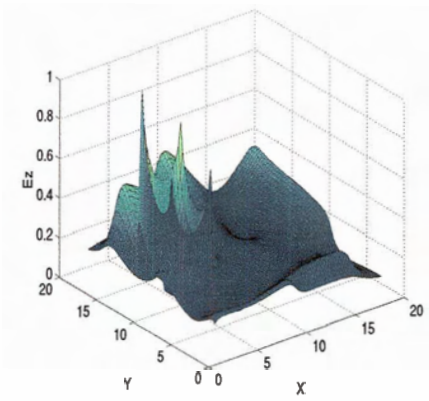

(g) 8.5 GHz

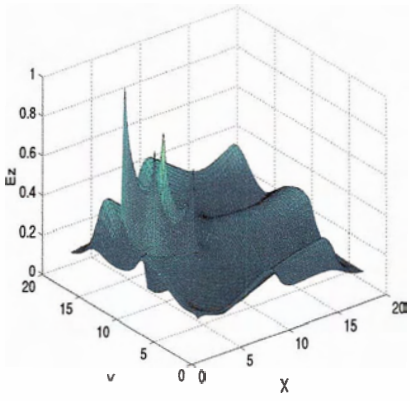

(h) 9.77 GHz

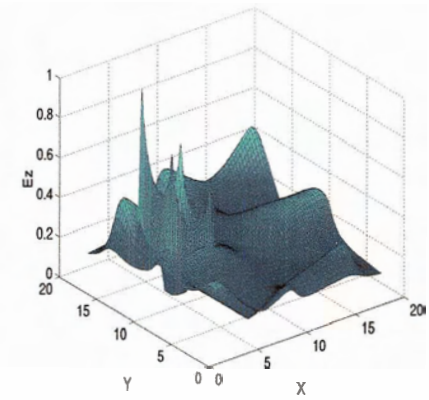

(i) 10.45 GHz

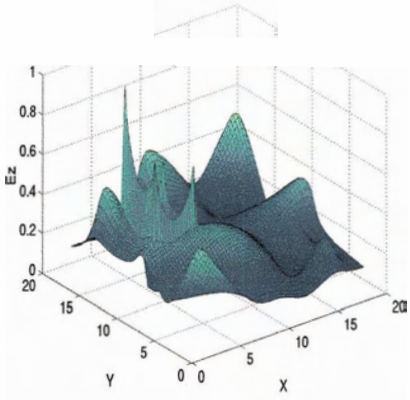

(j) 11.61 GHz

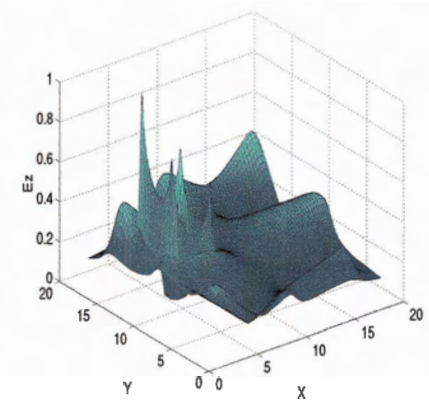

(n) 12.76 GHz

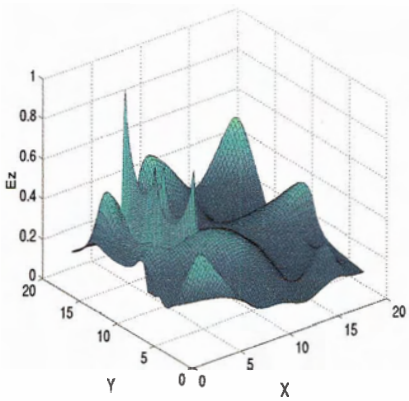

(o) 15.33 GHz

Figure 4. 9 Field distributions under the patch at different resonant frequencies.

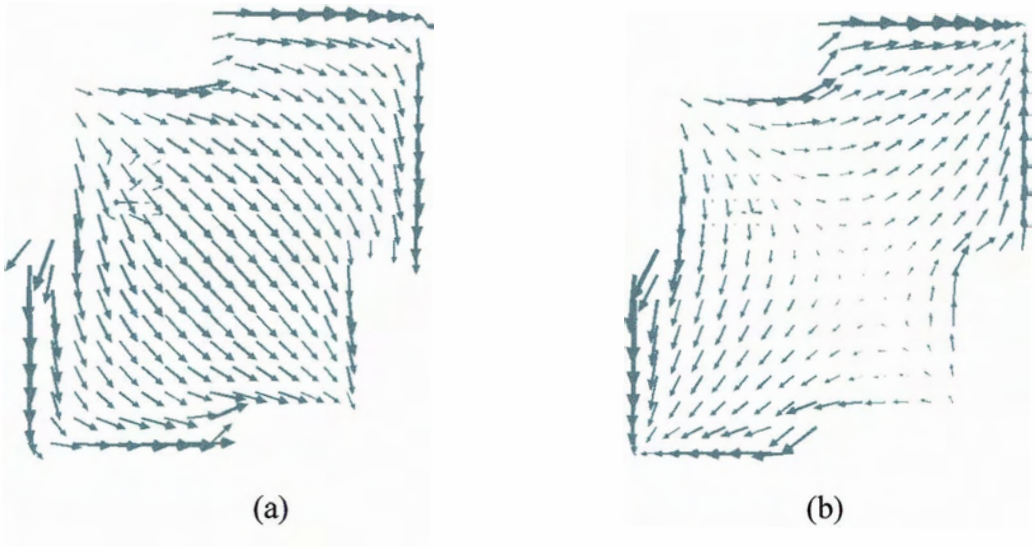

Figure 4. 10 Current distribution on the patch (a) 5.79 GHz (b) 7.85 GHz

To verify the simulation results, a prototype of the antenna was built. The antenna was built on RT/ Duroid 5870 substrate and measurements of the VSWR were made with Network Analyzer HP 8720C. Figure 4.11 shows the comparison between the measurement and simulation. It can be observed that the agreement between results from simulation and measurement is very good. A major reason behind the discrepancy between the measured results and simulation results is probably the misalignment between the two layers of the antenna. Another reason can be the deviation of the dimensions of the fabricated antenna from the specifications. The effect of the deviation of the specified dimensions from the specifications is examined in Section 4.2.

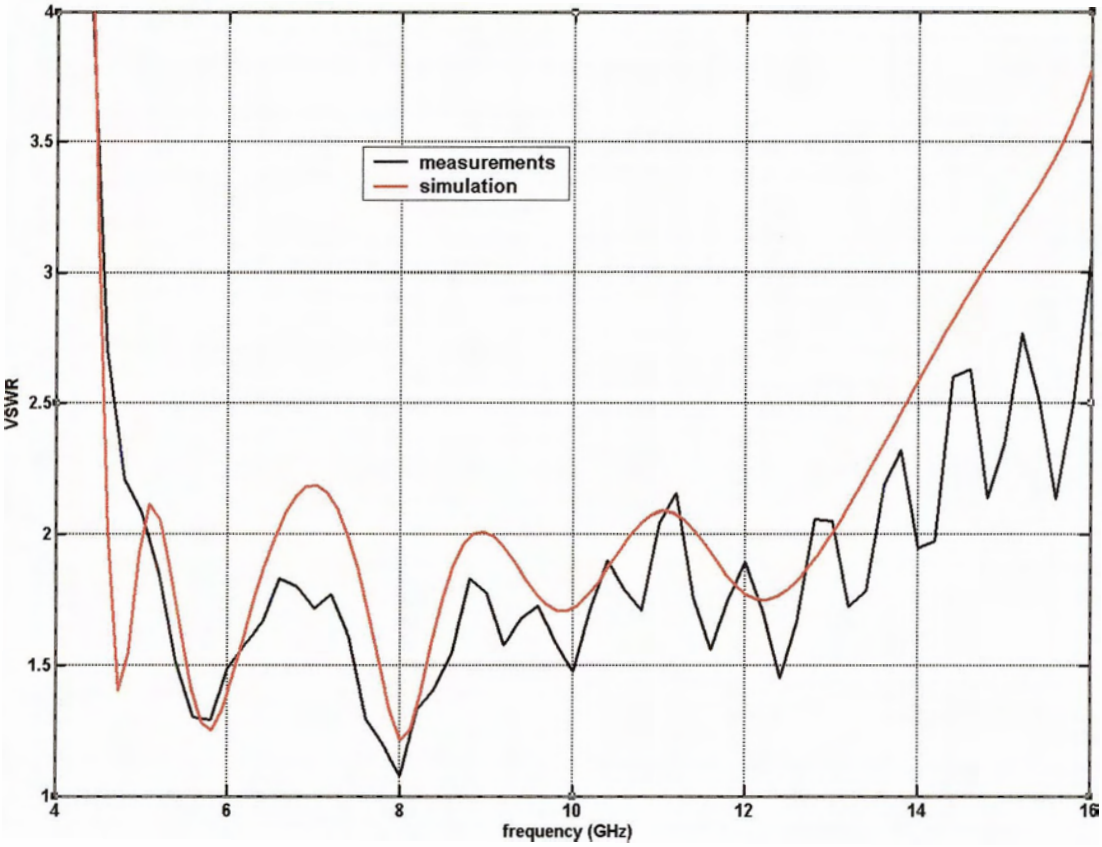

Figure 4. 11 Comparison of simulation and measured results for proposed antenna

Table 4.2 gives a summary of the characteristics of this antenna as compared to other broadband antennas described in recent publications. The proposed antenna has a wider impedance bandwidth compared to other antennas of similar surface area and thickness.

Here l is the antenna length, w is the antenna width, d is the diameter of circular patch, λ_0 free space wavelength at center frequency (for dual band antenna λ_0 is wavelength at the centre frequency of the lower band). For the circular patches instead of l/λ_0 the ratio d/λ_0 is calculated.

Table 4. 2 Comparison of the proposed antenna with other recently proposed antennas

Patch type	Band	Polarization	l/λ_0 or d/λ_0	w/λ_0	t/λ_0	VSWR 2:1	Gain (dB)
PIFA, meanders and rectangular [24]	Dual	Linear	0.11	0.073	0.025	7% 6.9%	1.0 - 2.7 1.0 - 2.1
Circular, shorting pin [5]	Single	Linear	0.135		0.063	6.8%	3.6 (max)
Circular, arc slots [25]	Single	Linear	0.44		0.042	10.4 %	4.8 (max)
Circular, two L-shaped slots [26]	Dual	Linear	0.35		0.09	12.4 % 21.5 %	7.2 (max) 7.1 (max)
E shaped [14]	Single	Linear	0.54	0.35	0.077	32.3 %	7.5 - 8.5
Two E patches, two feeds [6]	Dual	Linear	0.66	0.406	0.072	9 % 39.4 %	9.7 -11.2 5.4 - 6.5
Modified rectangular [23]	Single	Circular	0.22	0.22	0.045	13.9 %	4.6 (max)
Meander line probe [28]	Single	Linear	0.55		0.12	31 %	9.0 (max)
Aperture stacked [13]	Single	Linear	0.52	0.52	0.205	69 %	6.0 - 8.5
Modified bow-tie antenna [18]	Single	Linear	2.89	1.43	0.007	120.4%	1.0 – 3.0
H shaped, ring slot coupling [15]	Single	Linear	0.58	0.338	0.135	54 %	3.0 – 8.0
This antenna	Single	Dual	0.5	0.5	0.116	95.45%	2.5 - 6.5

The proposed antenna has a very wide bandwidth but within the band VSWR becomes greater than 2 at few frequencies. It is possible to sacrifice some bandwidth to obtain better VSWR. The antenna can also be designed for other frequency bands and on other substrates. To illustrate these points, two more examples (#2 and #3) are considered. In the first example, the antenna is re-designed on air substrate. In the second example (#3), the antenna is designed for low frequency operation. It has a bandwidth of 38.5 % (1,710 - 2,525 MHz). The antenna is designed to cover DCS (1,710-1,880 MHz), PCS

(1,885—1,990 MHz) and Bluetooth (2,400-2,485 MHz). Here bandwidth is sacrificed for compactness. The wideband antenna (#1) has a size of 0.5 λ_0 and thickness 0.11λ_0. The low frequency antenna (#3) has a size of 0.33 λ_0 and thickness 0.068λ_0. The VSWR and gain performance for antenna (#2) are shown in Figure 4.12 and Figure 4.13 and for antenna (#3), are shown in Figure 4.14 and Figure 4.15 respectively. Table 4.3 gives the dimensions of the different antennas that have been analyzed. Table 4.4 summarizes their performances.

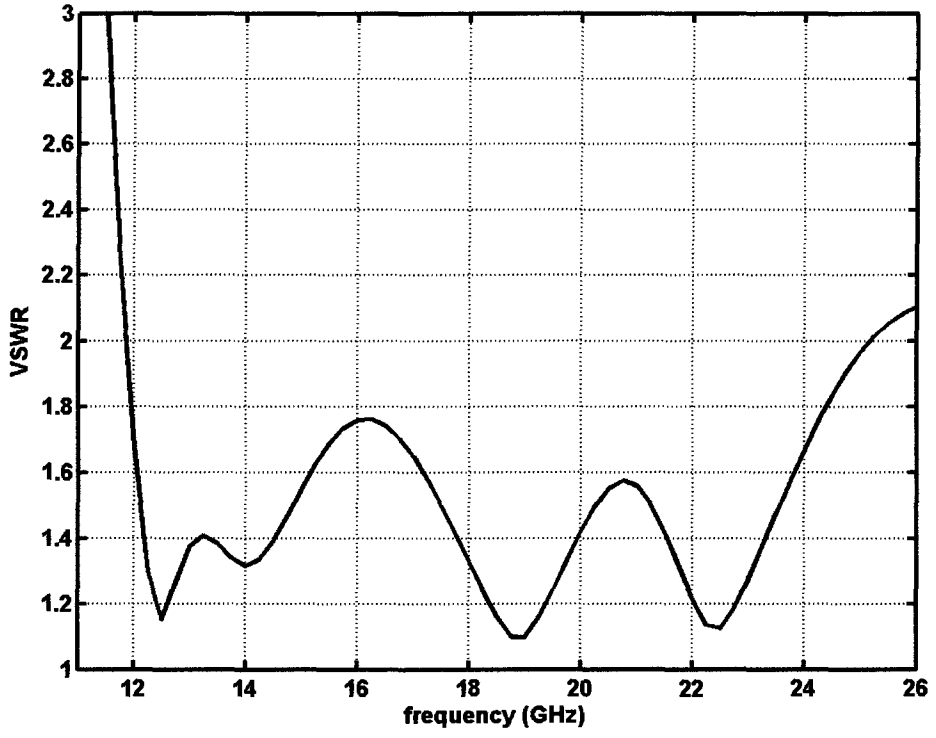

Figure 4. 12 VSWR of antenna #2 (VSWR < 2 for 11.82-25.25 GHz)

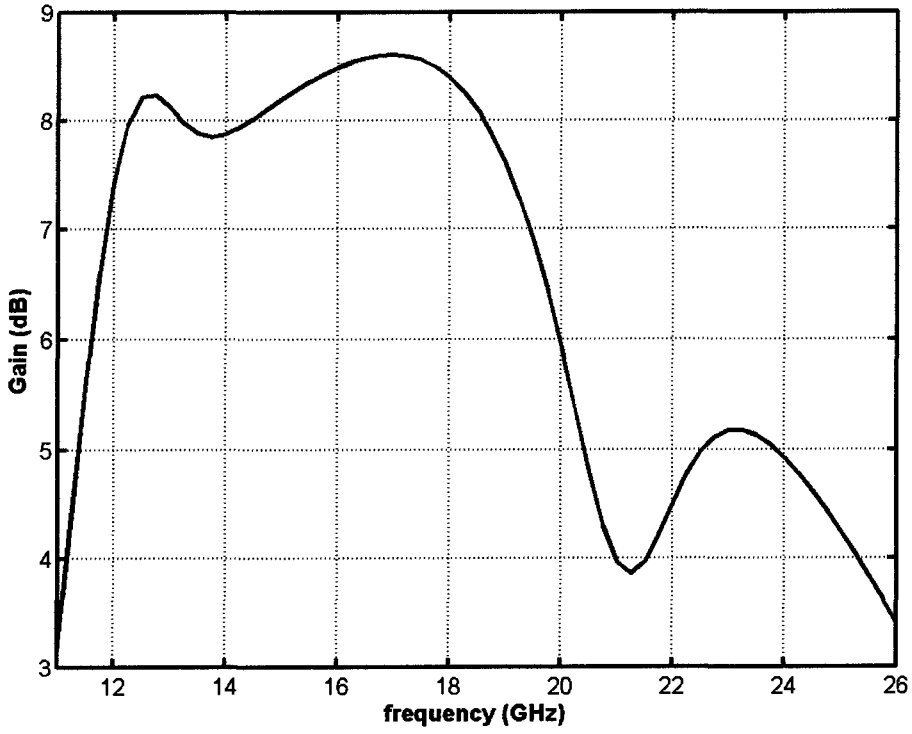

Figure 4. 13 Gain of antenna #2

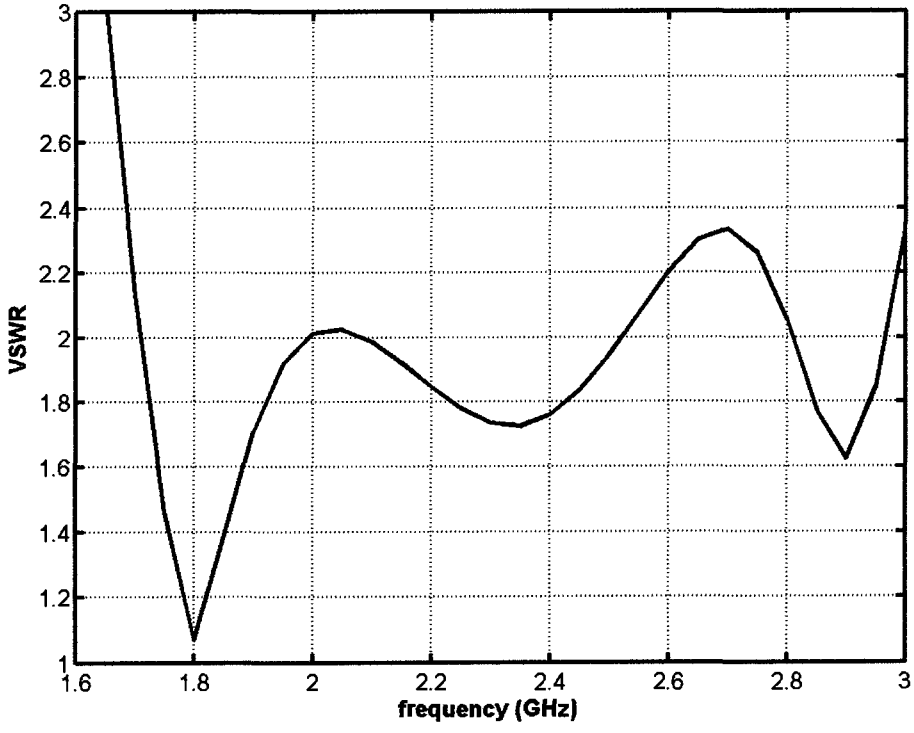

Figure 4. 14 VSWR of antenna #3 (VSWR < 2 for 1.71 - 2.53 GHz)

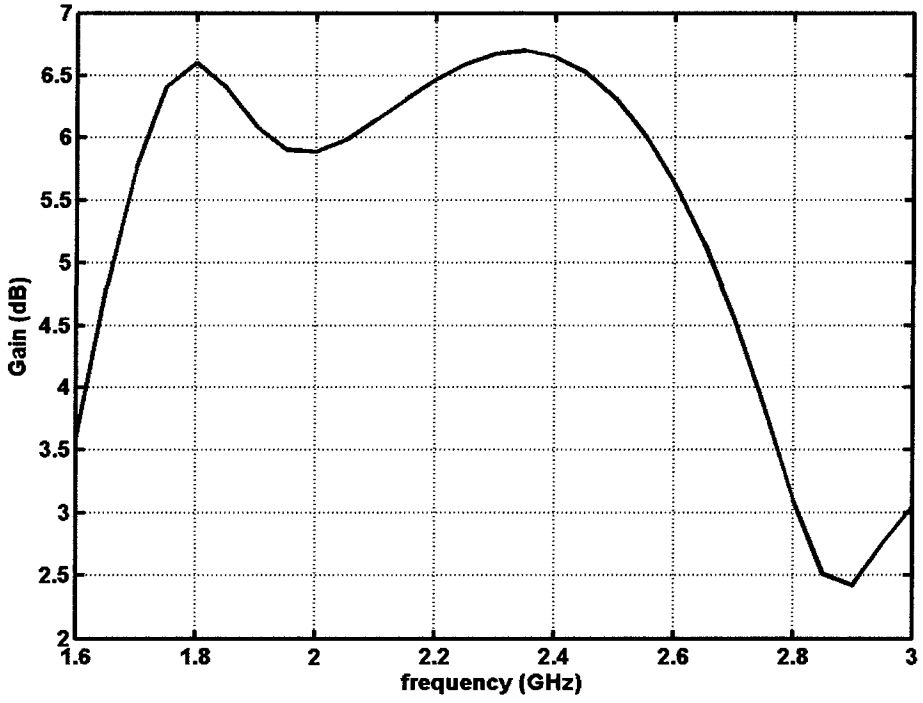

Figure 4. 15 Gain of antenna #3

Table 4. 3 Dimensions of the various antennas

Antenna	W_1 (mm)	W_2 (mm)	W_3 (mm)	S_1 (mm)	S_3 (mm)	h_1 (mm)	h_2 (mm)	ε_r (mm)
#1	8	13.5	10	7	7.5	0.8	3.175	2.25
#2	23.5	39	24	18.5	18	0.75	9	2.25
#3	3.75	7	5.25	2.75	7	0.25	1.6	1.0

Table 4. 4 Performance of the various antennas

Antenna	Frequency range (GHz)	VSWR ≤ 2 BW (%)	Gain (dB)
#1	4.60 - 13.01	95.45	2.5 - 6.5
#2	11.82 - 25.25	70.27	4.0 - 8.5
#3	1.71 - 2.53	38.10	5.75 - 6.75

4.2 Sensitivity analysis

The antenna gives optimum performance for a particular choice of antenna dimensions. During the fabrication the dimensions will not exactly match the specifications and the performance may be different from the expected one. It is expected that the antenna performance will not vary significantly for a small change of antenna dimensions. To examine the sensitivity of the proposed antenna, the antenna dimensions are varied by a small amount and the variation in VSWR bandwidth is observed. Table 4.5 summarizes the results.

Table 4. 5 Effect of variation of dimensions on antenna peformance

Dimension under investigation	change in dimension (%)	VSWR bandwidth (%)	Change in VSWR bandwidth (%)
W_1	5	97.3 % (4.75 – 13.75 GHz)	2
	-5	86.3 % (5.54 – 13.6 GHz)	-9
W_2	5	97.1 % (4.5 – 13 GHz)	2
	-5	84.8 % (5.5 – 13.6 GHz)	-10
W_3	5	84.9 % (5.25 – 13 GHz)	-10
	-5	95.9 % (4.75 – 13. 5 GHz)	0.4

The change of dimensions affects the antenna performance. However, for a small change in antenna dimensions, the antenna still retains very wide VSWR bandwidth

4.3 Integration of the Antenna with EBGs

Recently, enhancing performance of microstrip anetnnas using EBGs. [38], [29] has shown significant promise. The VSWR bandwidth of the proposed antenna is sufficient for most applications. The gain of the antenna is good but decerases at higher

frequencies. Thus investigation has been made regarding the possibility of enhancing the antenna performance further by using EBGs.

The proposed antenna has very wide bandwidth. It is not possible to design compact EBG with such large bandwidth. Thus, EBG is designed to have a stop band around the frequency where the antenna performance is the worst. The antenna has a rapid decrease in gain in the bore sight near 8 GHz. Therefore, the EBG is designed to have a stop-band near 8 GHz. The proposed antenna is a two layer structure and for ease of fabrication, the EBGs are placed in the lower layer. The permittivity of substrate is 2.35. Hexagonal EBG is chosen because of its ability to prevent surface wave propagation in any direction. The EBG cell has equal sides of length 1.4 mm. The phase of the reflection coefficient of waves incident at the normal angle to the EBG surface is shown in Figure 4.16.

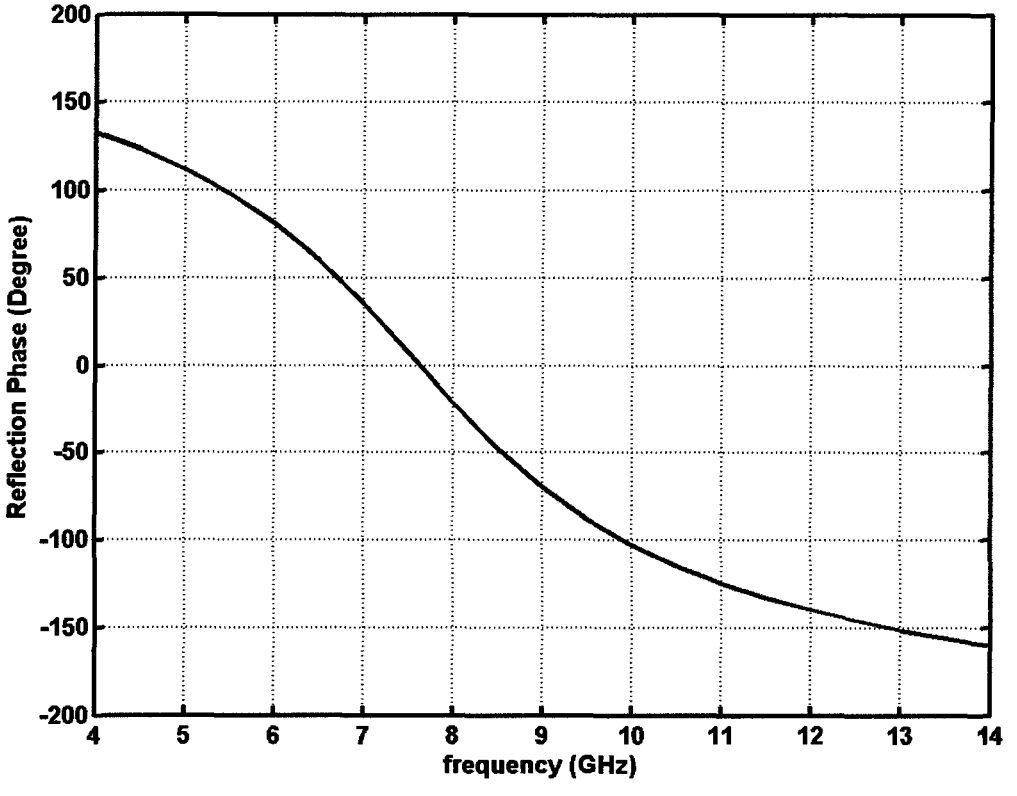

Figure 4. 16 Phase of the reflection coefficient for the EBG

A parametric study was performed to determine the gap between EBG layers and antenna and the number of EBG layers necessary to get improvement in gain and maintain the VSWR. The following cases are considered:

Case 1: one EBG layer placed 3.5 mm away from antenna
Case 2: two EBG layers placed 3.5 mm away from antenna
Case 3: one EBG layer placed 5.5 mm from antenna
Case 4: two EBG layers placed 5.5 mm from antenna
Case 5: three EBG layers placed 5.5 mm from the antenna

The VSWR performance of the antenna with different EBG configurations is shown in Figure 4.17. As can be seen, the VSWR bandwidth is significantly reduced when EBG is placed around the antenna. However, even this reduced bandwidth is sufficient for many practical applications. The reduction in bandwidth is more pronounced when the number of EBG layers is increased or the spacing between the EBG and the antenna is reduced. This is expected since the EBGs block the propagation of surface waves and form a resonant cavity. When the number of EBG layers is increased or the EBGs are placed closer to the antenna, quality factor of the cavity increases and bandwidth is reduced.

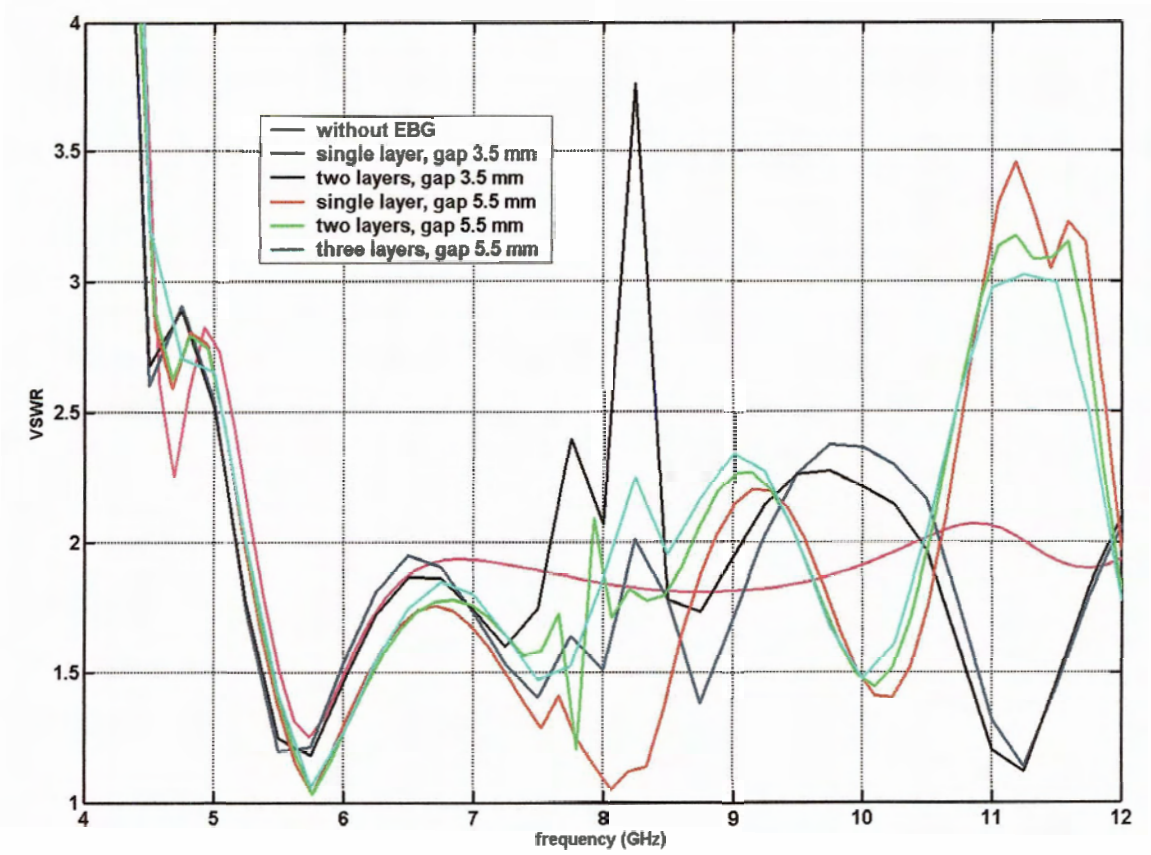

Figure 4. 17 Modeled VSWR performance of the antenna with EBGs

Prototypes were built with EBGs placed around the antenna and VSWR was measured with network analyzer HP 8720 C. Figure 4.18 shows the comparison of VSWR obtained from simulation and measurements for the case of 2 layers of EBGs placed 5.5 mm away from the antenna. The results are in reasonably close agreement. The discrepancy between the two at some frequencies may be resulting from the misalignment of the two layers of the antenna. The measurement results for the other structures are given in Appendix C.

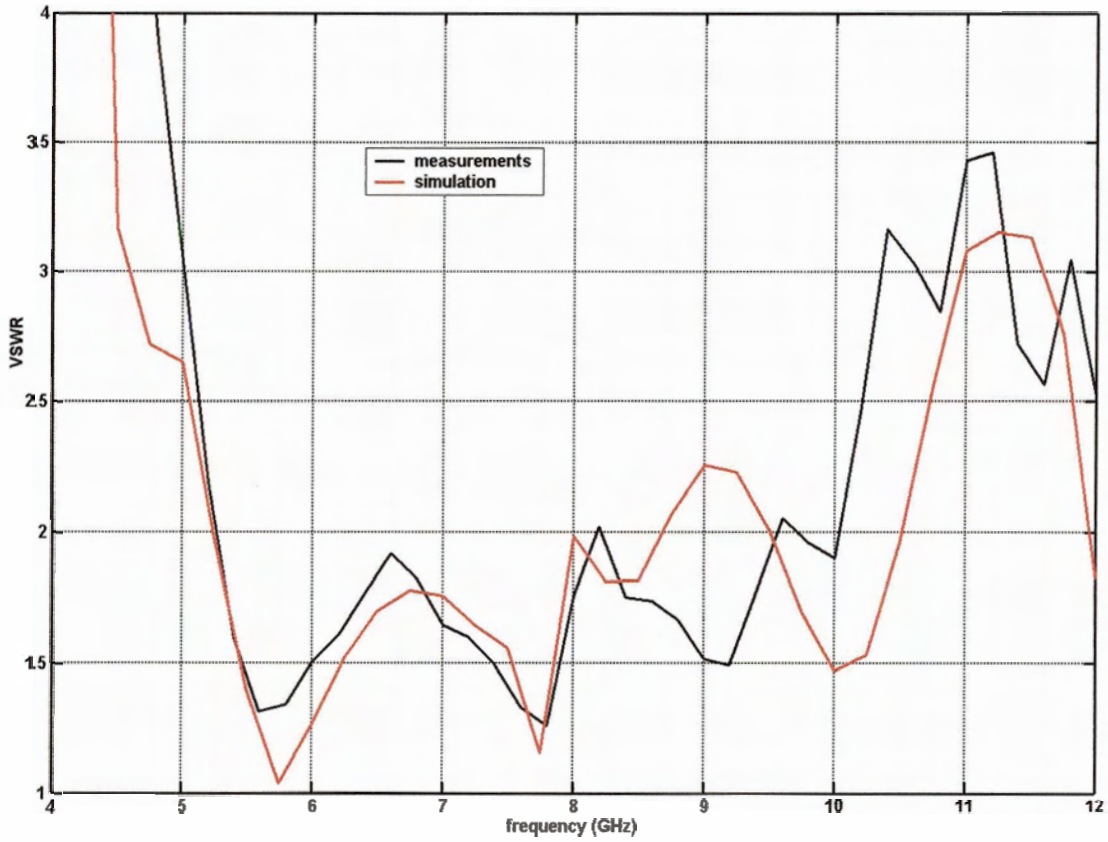

Figure 4. 18 Comparison of simulation and measured results for the proposed antenna with 2 layers of EBG placed 5.5 mm away from the antenna

The gain in three different planes is shown in Figure 4.19, Figure 4.20 and Figure 4.21. Up to 8 GHz the application of EBGs does not show any enhancement of gain. In fact, gain is slightly reduced compared to the reference antenna. However, above 8 GHz the antenna shows much higher gain compared to the reference antenna. The gain plots show very sharp dips at 8 GHz when the EBG layers are close to the antenna. Increasing the number of EBG layers beyond two does not increase the gain significantly. The best performance is obtained by placing two layers of EBG around the antenna at a distance of 5.5 mm from it (curves designated by the green line).

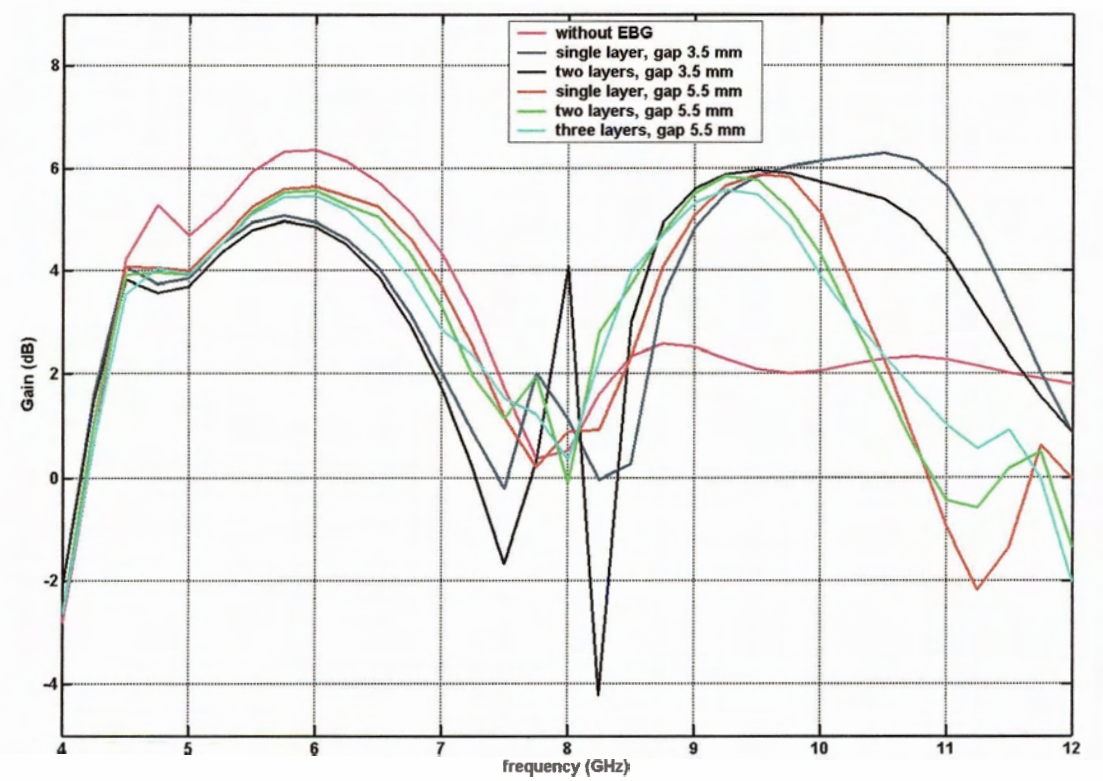

Figure 4. 19 Gain of the antenna in the θ=0° and ϕ=0° direction

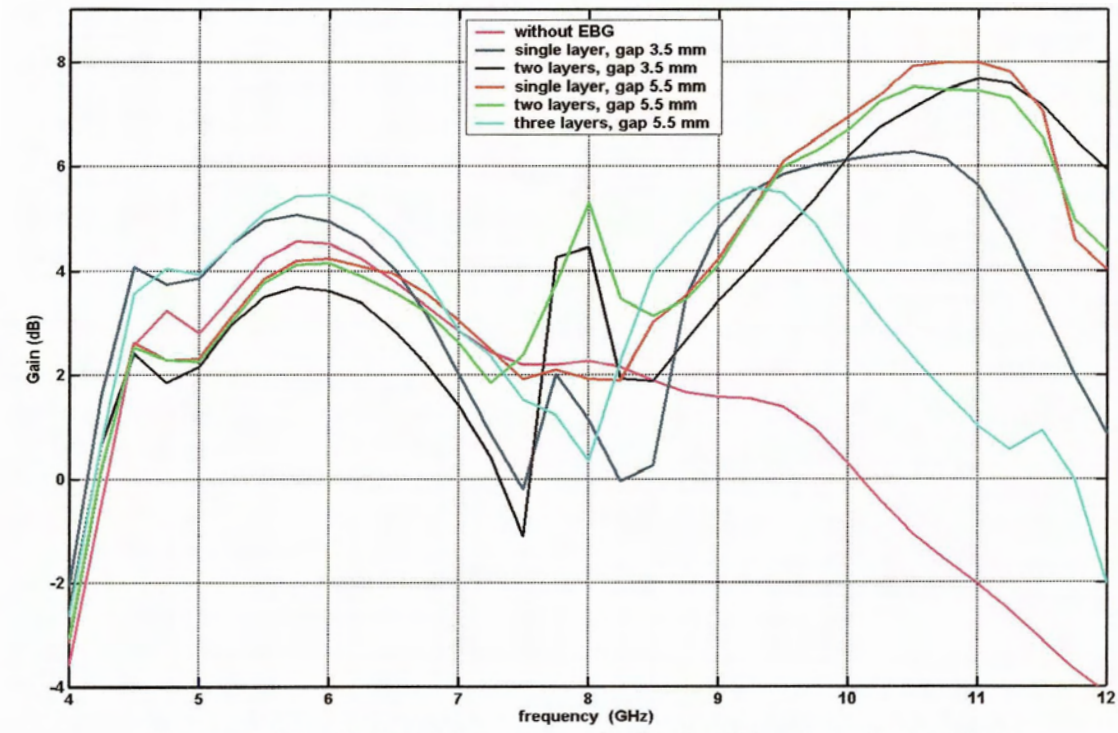

Figure 4. 20 Gain of the antenna in the θ=30° and ϕ=0° direction

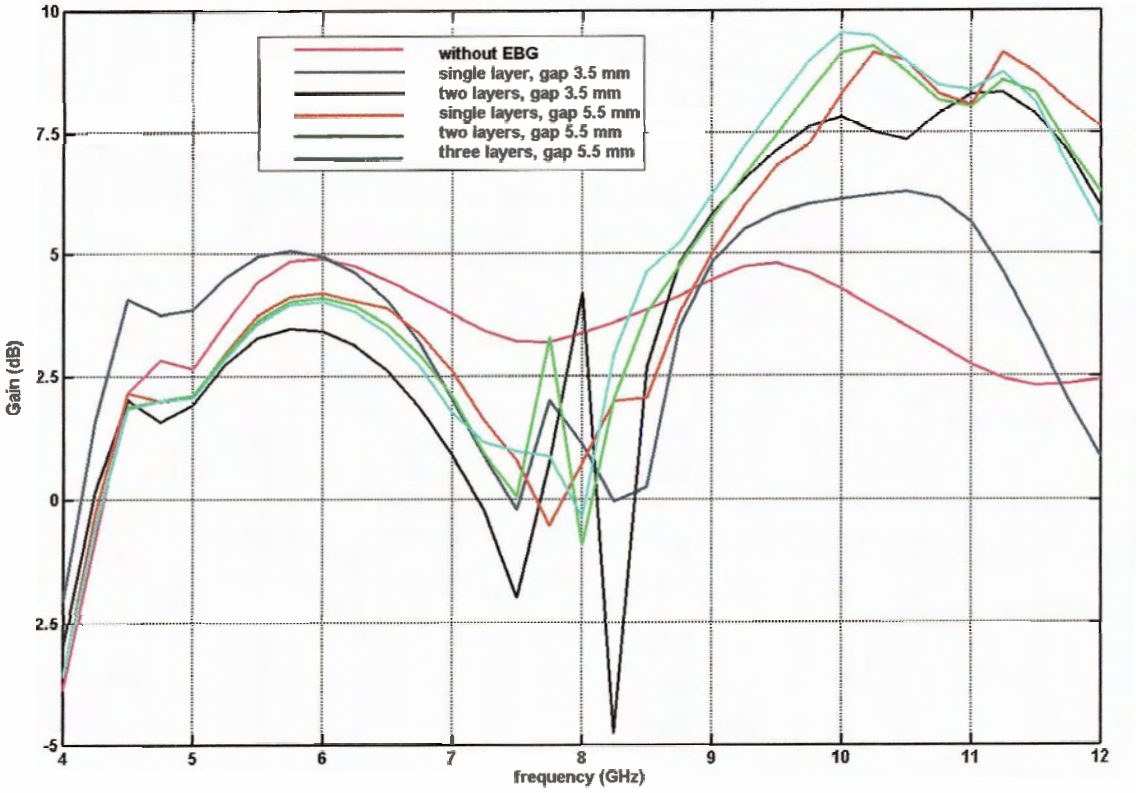

Figure 4. 21 Gain of the antenna in the θ=30° and ϕ=45° direction

4.4 Conclusions

A novel microstrip antenna has been designed and analyzed. The antenna is compact, easy to fabricate and provides good gain. The simulation results are verified by measurement. The use of EBG can further enhance the performance of the antenna. Table 4.5 summarizes the effect of EBGs around the antenna (2 layers of EBG 5.5 mm away from antenna).

Table 4. 6 Comparison of antenna performance with and without EBGs

Antennas	VSWR ≤ 2.2		Gain (dB) in different planes		
	Measurements	Simulations	$\theta = 0^0$ $\phi = 0^0$	$\theta = 30^0$ $\phi = 0^0$	$\theta = 30^0$ $\phi = 45^0$
Without EBG	94.3 % (5.1 to 14.2 GHz)	95.5 % (4.6 to 13.01 GHz)	0.4 to 6.4	-6 to 4.3	2.4 to 4.98
Two layers of EBG	64.1 % (5.2 to 10.1 GHz)	68.7 % (5.18 to 10.6 GHz)	-0.2 to 5.9	2.4 to 6.75	-1 to 9.3

The main advantage of the antenna is very wide impedance bandwidth. A serious limitation, at least in some applications, is the change in polarization as a function of frequency. However, for antennas operating in multi-path environments this limitation may no longer apply. Thus, this antenna can be a very good candidate for some applications in wireless communications.

5. Broadband Loop Antenna

5.1 Introduction

With the widespread use of cell phones, there is demand for antennas that have sufficient bandwidth to cover several mobile frequency bands. It is also important to minimize the electromagnetic interaction between the user and the antenna to avoid possible health hazard. Many different antennas have been investigated for application in handsets. Loop antennas are very easy to built and when they are built on a substrate, they are also mechanically strong. Applications of loop antennas in mobile devices have been previously considered [60]. However, conventional loop antennas have less than 10% bandwidth of VSWR < 2 [2]. A modified loop antenna can offer 24% bandwidth [2]. The gain of the antenna, however, is low. Also, when it is placed near the user's head, the latter absorbs a significant amount of radiated power. The absorbed power may exceed the prescribed limits that are considered to prevent health hazard. Furthermore, it reduces the radiation efficiency of the antenna.

The structure reported in [2] would be more compact, if the antenna could be placed on the handset box. Directly placing the antenna near the box surface is not an acceptable solution, since the surface is metallic, and thus acts as an electric wall. On the other hand, the antenna can be placed on an EBG layer, since it acts as a magnetic wall in its stop band. This makes the structure more compact and also the radiation inside user's head will be reduced.

This chapter reports an investigation of the antenna reported in [2] placed on an EBG surface. The antenna dimensions are optimized to obtain good performance. The antenna performance in terms of VSWR, directivity and far field radiation patterns is investigated. In house FDTD code Totem is used for all the simulations. Because of a non-planar structure of the antenna, the available MoM codes are not satisfactory for modeling of this antenna.

5.2 Design of an EBG Structure for the Antenna

Because of the small size of handheld communication devices (e.g. telephones, PDAs) an EBG structure used for improving antenna performance should be sufficiently compact and it should have a reasonably wide bandwidth. There are many different EBGs described in literature that can be used for realizing a magnetic surface [29], [61,62]. Summary data for representative structures are listed in Table 5.1. All these EBGs are designed on a substrate with ε_r=4.4.

Table 5. 1 Comparison of different EBGs

Type	Cell size at 2 GHz (Square)	Period	Height	Bandwidth
Mushroom (double layer) [29]	6mm	$0.04\lambda_0$	$0.013\lambda_0$	8.9%
Mushroom (single layer) [29]	14.7mm	$0.098\lambda_0$	$0.065\lambda_0$	38.4%
Slotted rectangular [61], [62]	11.1mm	$0.074\lambda_0$	$0.0629\lambda_0$	33.6%

The slotted rectangular EBG is a good compromise between bandwidth and size. This structure, shown in Figure 5.1 is selected.

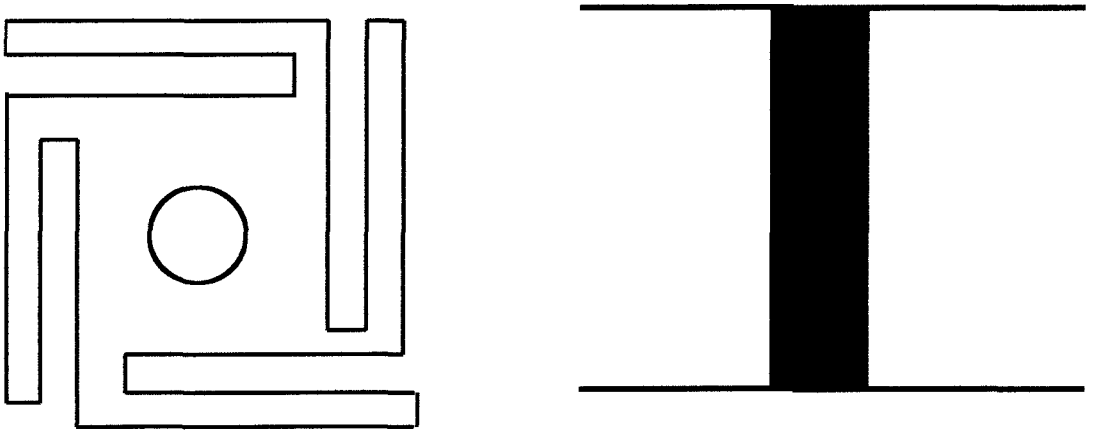

Figure 5. 1 Slotted EBG structure (a) top view (b) side view.

The EBG is designed to have a stop band centered around 2.16 GHz. The reflection phase of the EBG is shown in Figure 5.2. Reflection phase is between -90° and 90° from 2 to 2.3 GHz.

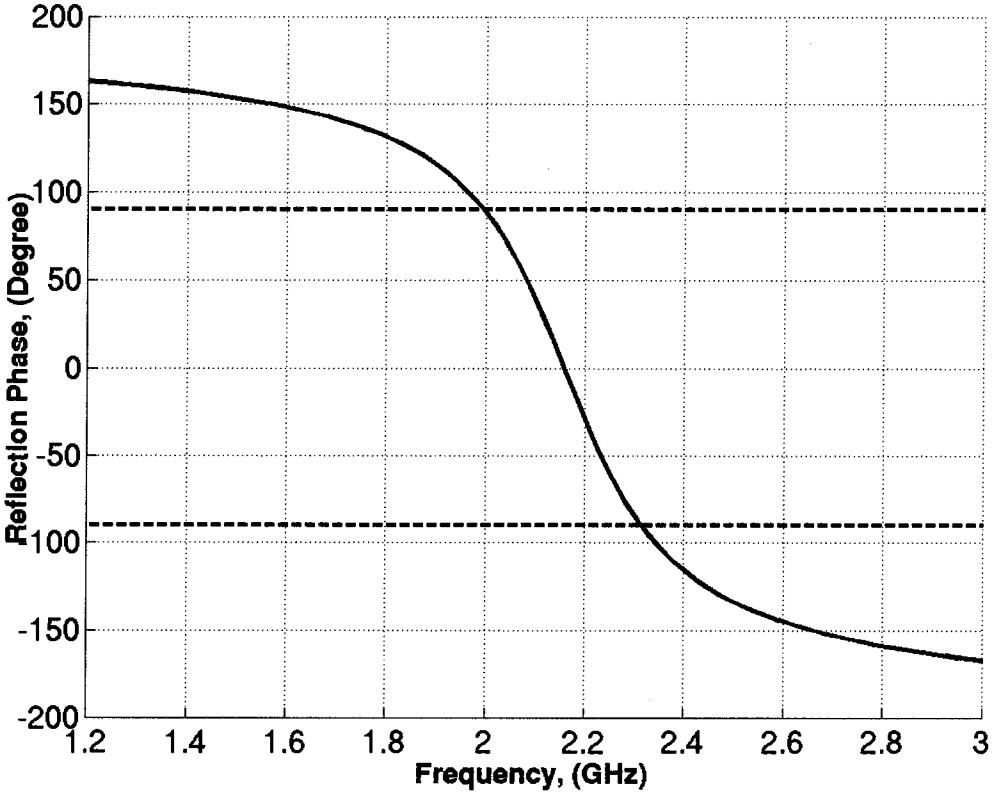

Figure 5. 2 Phase of reflection coefficient for the slotted EBG structure

5.3 Description of the Antenna

Figure 5.3 shows the antenna configuration reported in [2]. The structure consists of two monopoles. A coaxial probe excites one of the monopoles, and the other one is a parasitic monopole coupled to the excited one by a small gap. The monopoles have different lengths, which is essential for achieving wide impedance bandwidth.

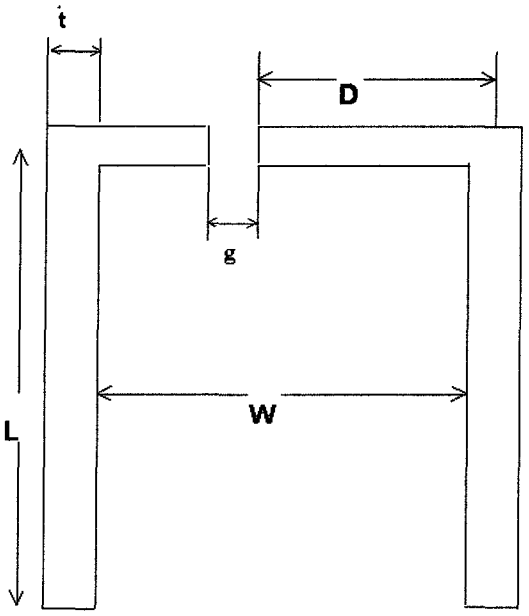

Figure 5. 3 Structure of the modified loop antenna

In [2] the antenna is optimized without EBGs. When the antenna is placed above the EBGs, there is a complex interaction between the antenna and the EBGs. Therefore, it is necessary to optimize the antenna dimensions again to achieve the required performance.

For the modeling, FDTD code is used. The computational volume is truncated with PML of 7 layers. A uniform grid of 0.25 mm is used in x and y directions; in the z direction grid ranges from 1 mm to 2 mm and the gradual changes are within a limit of 1:1.2. The antenna is excited by a 50-ohm source with a Gaussian pulse centered at 2 GHz and having a bandwidth of 2 GHz. The number of time steps is 3000 to ensure that the pulse amplitude decays to a small fraction of its peak value.

Two parameters, gap between the two monopoles (g) and the width of the monopoles (t) strongly influence the input impedance. Therefore, a parametric study is performed to investigate their effects on the input impedance. The results are shown in Figure 5.4 for the resistance and in Figure 5.5 for the reactance. The input reactance is mostly

inductive. This is expected since the capacitance introduced by the gap does not compensate for the loop inductance for long loop widths.

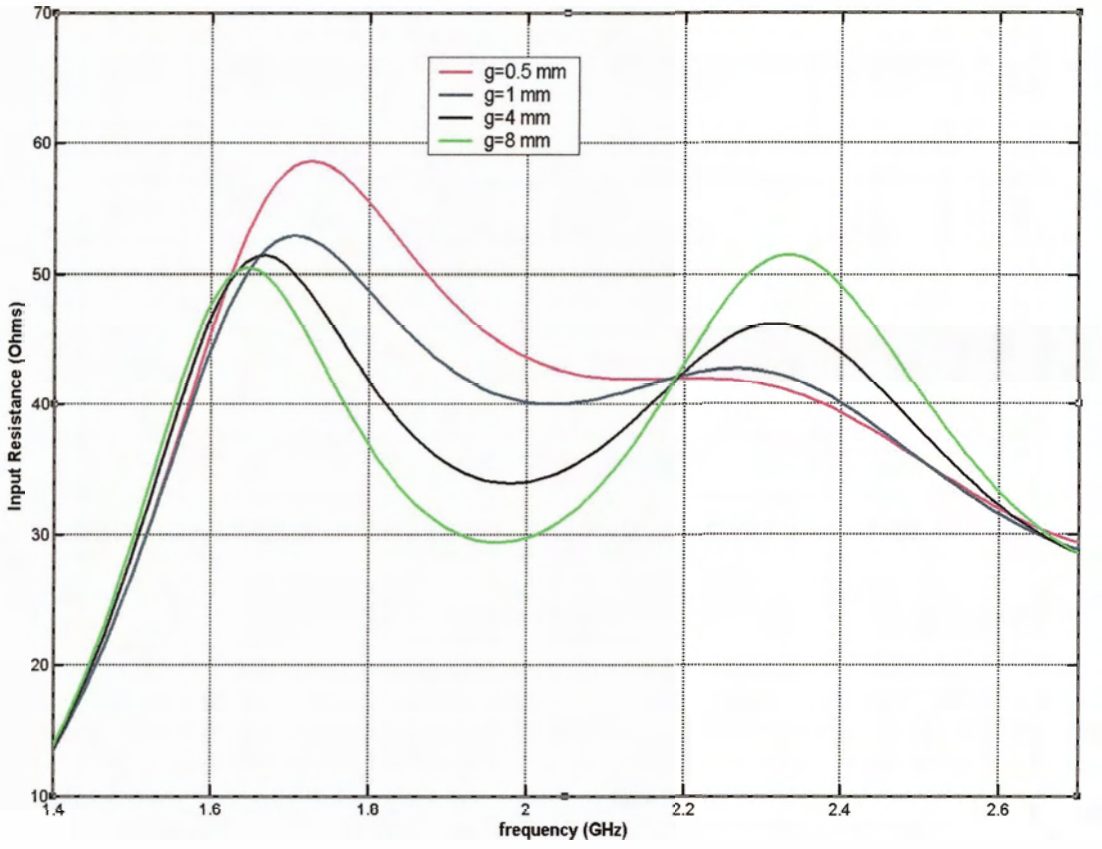

(a)

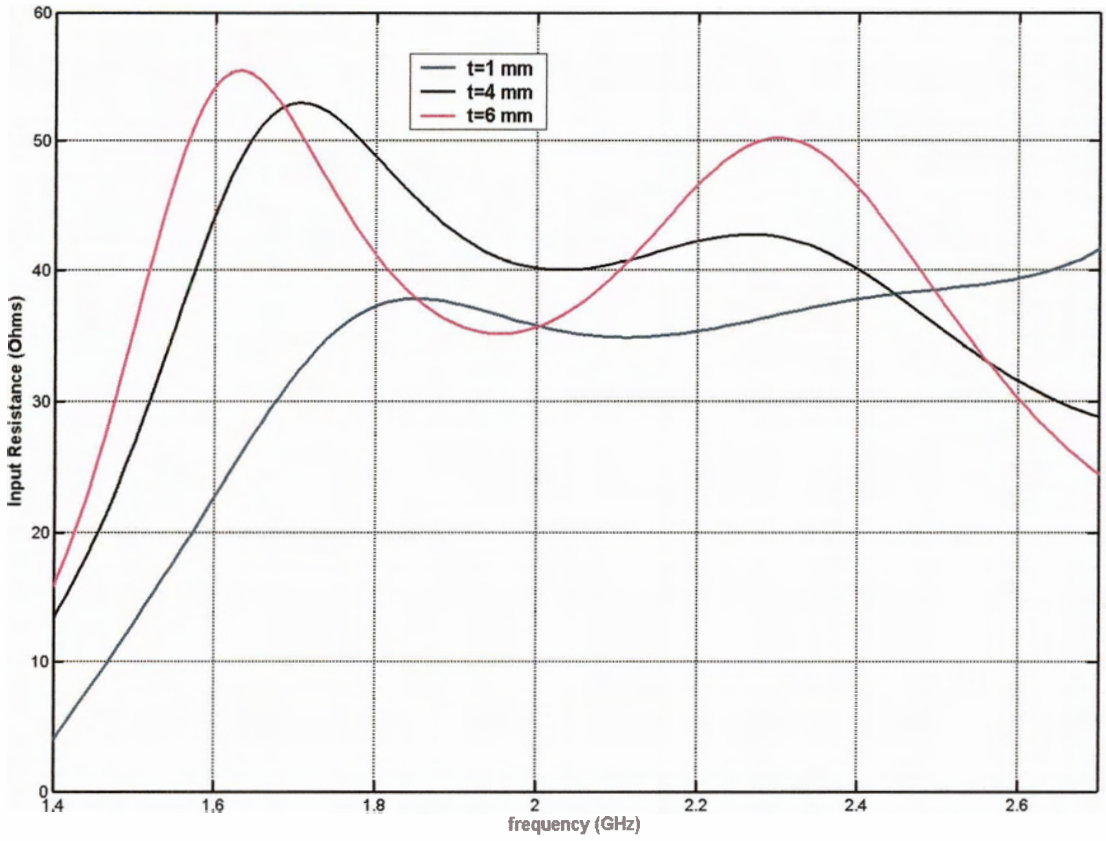

(b)

Figure 5. 4 Effects of gap dimension and antenna width on its input resistance (a) gap g varied from 0.5 mm to 8 mm, with L=24 mm, D=14.5 mm, t=3.25 mm, W=16 mm (b) width t varied from 1 mm to 6 mm with L=24 mm, D=14.5 mm, g=1 mm, W=16 mm.

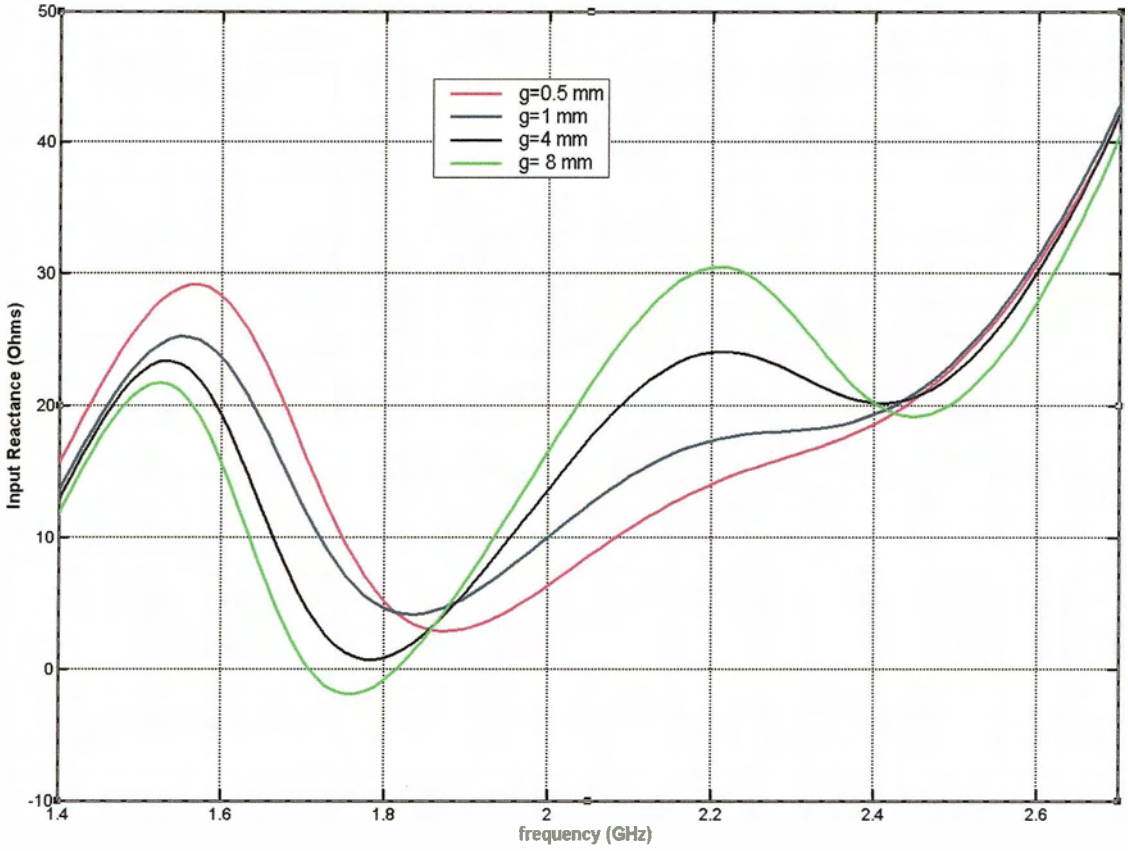
g=0.5 mm
g=1 mm
g=4 mm
g= 8 mm
Input Reactance (Ohms)
frequency (GHz)
50
40
30
20
10
0
-10
1.4
1.6
1.8
2
2.2
2.4
2.6

(a)

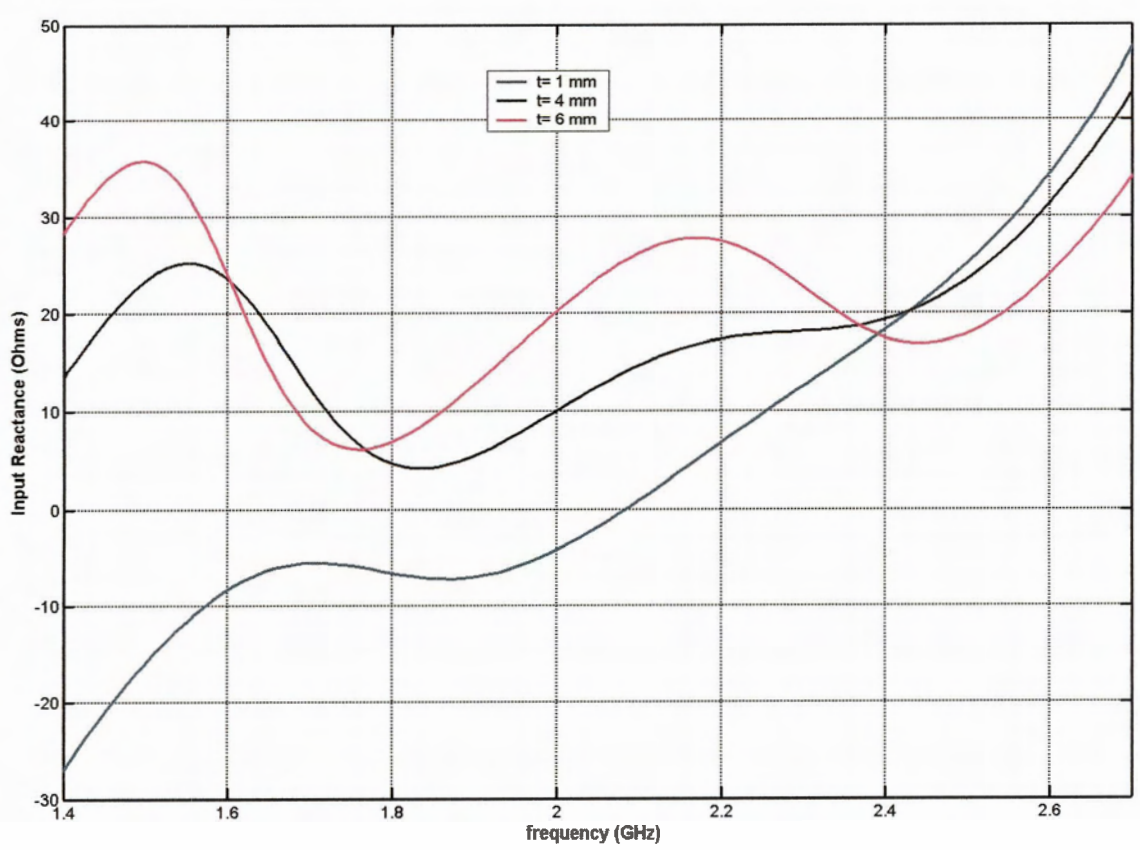

(b)

Figure 5. 5 Effects of gap dimension and antenna width on its input reactance (a) gap g varied from 0.5 mm to 8 mm, with L=24 mm, D=14.5 mm, t=3.25 mm, W=16 mm (b) width t varied from 1 mm to 6 mm with L=24 mm, D=14.5 mm, g=1 mm, W=16 mm

Based on the parametric study, the following antenna dimensions are chosen L=24, t=3.25 mm, g=0.75 mm, D=14.5 mm, W=16 mm. The antenna is placed 1 mm above the EBG surface. The EBG is built on a substrate with ε_r=4.4 and thickness 5 mm. Two EBG cells are placed at each side of the antenna. The structure is shown in Figure 5.6. The box on which the antenna and the EBGs are placed has dimensions of 80 mm (length), 60 mm (width), and 16.5 mm (thickness).

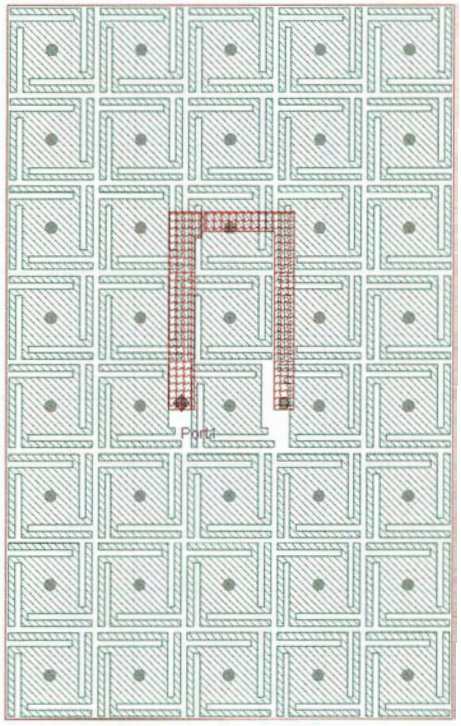

Figure 5. 6 Modified loop antenna integrated with EBGs

5.4 Modeling Results

The VSWR of the antenna is shown in Figure 5.7. The VSWR bandwidth is 46.83 % (1.57-2.53 GHz). The bandwidth is sufficient to cover four services, namely DCS-1800 (1.71-1.88 GHz), PCS (1.85-1.99 GHz), IMT-2000 (1.885-2.17 GHz) and Bluetooth (2.4-2.485 GHz).

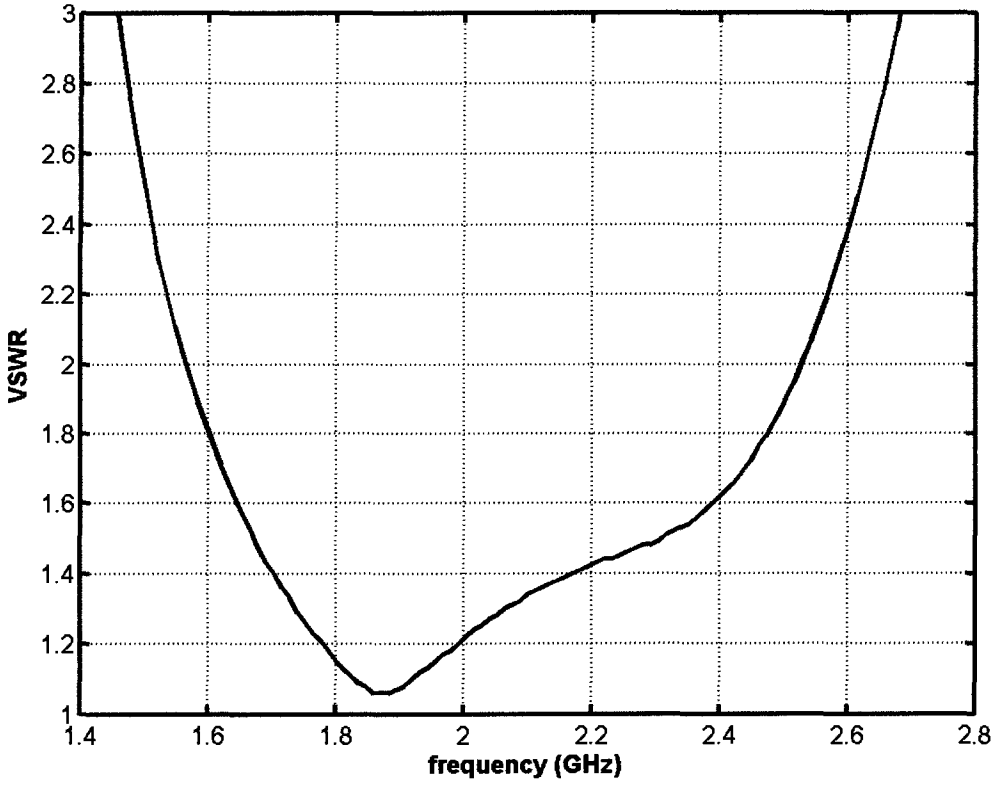

Figure 5. 7 VSWR performance of the antenna

The directivity of the antenna is shown in Figure 5.8. The antenna directivity should be sufficient for mobile communication systems.

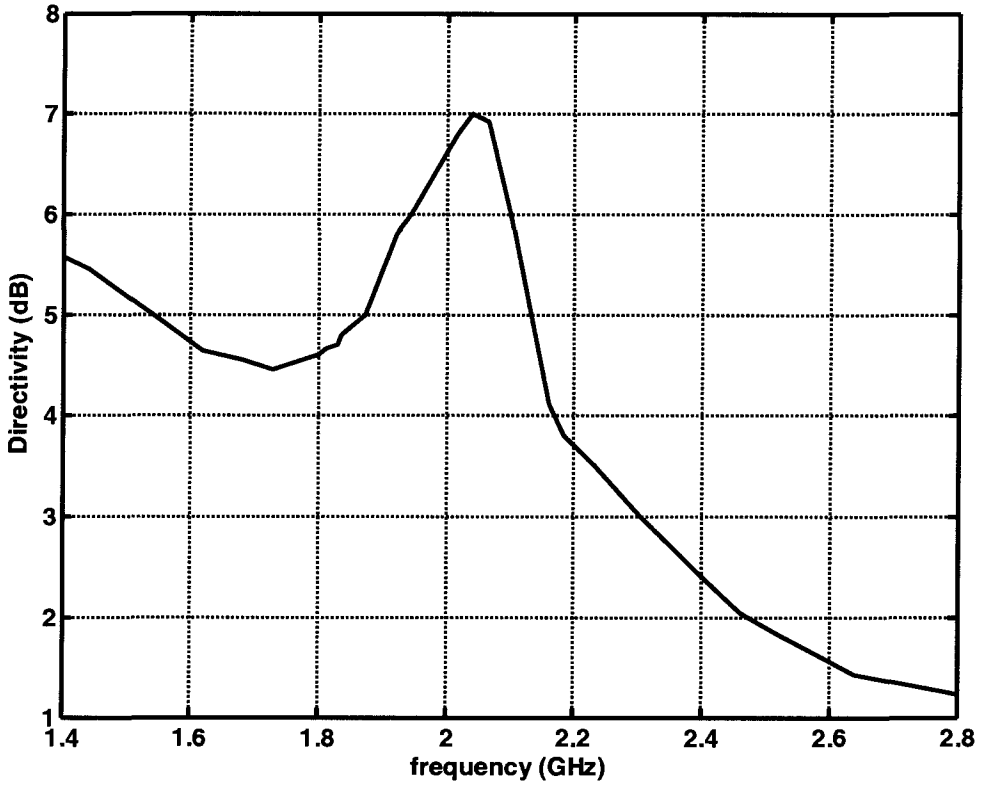

Figure 5. 8 Directivity of the antenna

The radiation patterns at a few frequencies within the antenna operating frequency band are shown in Figure 5.9. The front to back ratio is around 10 dB. This is expected, as the EBG surface blocks radiation in the backward direction. It also agrees with previously published results for a narrow-band antenna placed on the EBG surface [29].

At 1.7 GHz

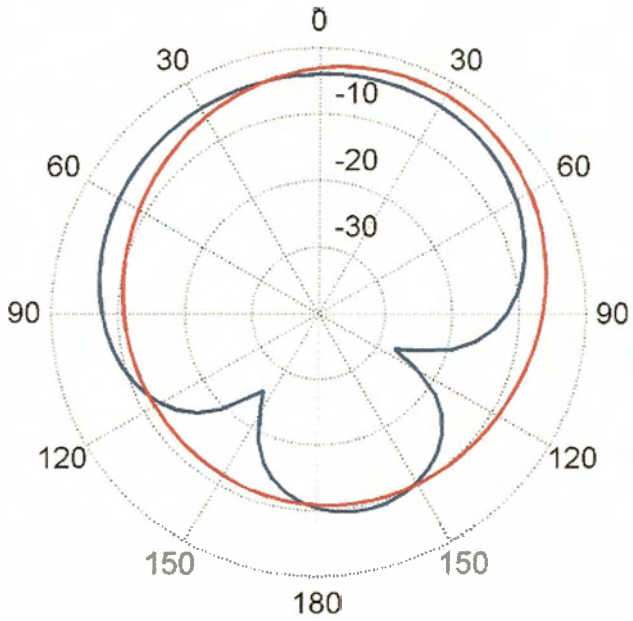

At 1.85 GHz

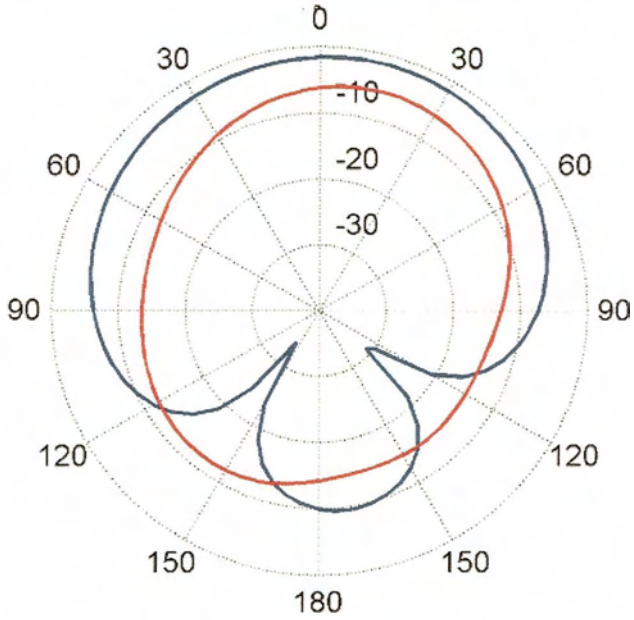

At 2 GHz

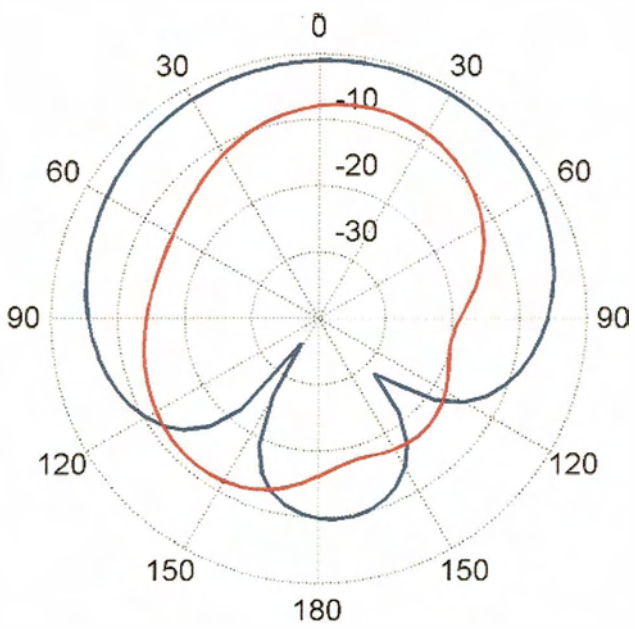

At 2.2 GHz

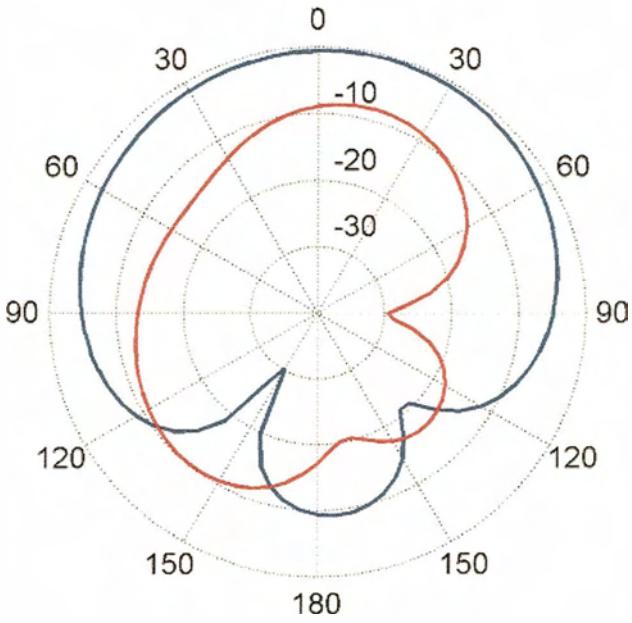

At 2.3 GHz

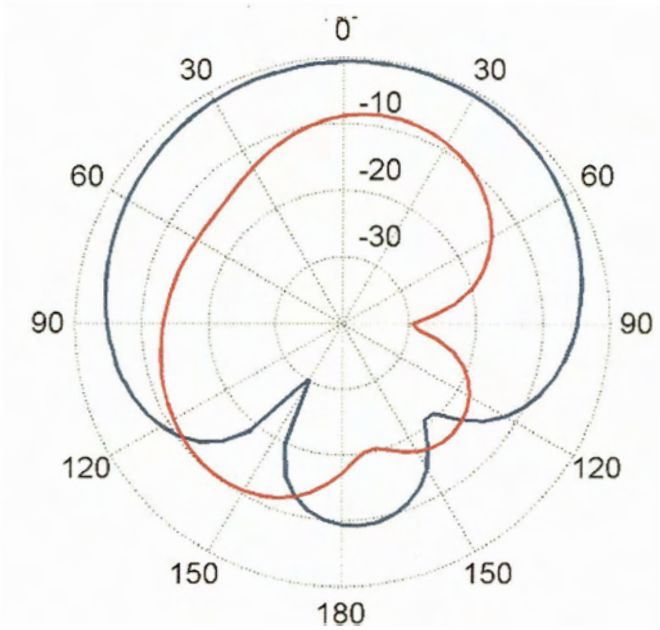

At 2.5 GHz

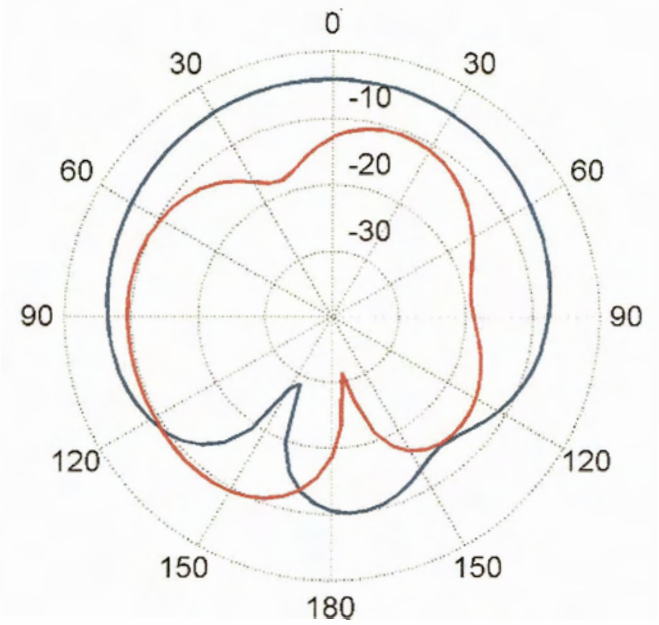

Figure 5. 9 Radiation patterns of the antenna; red line for E_ϕ and green line for E_θ (all patterns normalized to the maximum).

5.5 Sensitivity analysis

The antenna dimensions after optimization are L=24 mm, D=14.5 mm, t=3.25 mm, W=16mm. The antenna dimensions are varied to observe its effect on antenna performance. Two parameters are varied - the gap between two arms of the antenna and the width of the antenna. Table 5.2 summarizes the effect of changing the gap and Table 5.3 summarizes the effect of changing antenna width.

Table 5. 2 Effect of changing the gap (g) on antenna performance

Gap between two arms (g)	VSWR bandwidth (%)	Change in VSWR (%)
1 mm	46.1 % (1.3 – 2.1 GHz)	-1.5
4 mm	47.1 % (1.3 – 2.1GHz)	0.6
8 mm	50.3 % (1.28 – 2.15 GHz)	7

Table 5. 3 Effect of changing antenna width on antenna performance

Width of the antenna	VSWR bandwidth (%)	Change in VSWR (%)
1 mm	44 % (1.63 – 2.55 GHz)	-6
4 mm	45 % (1.6 – 2.53 GHz)	-3.9

From the tables it is clear that the antenna performance is not seriously affected by minor changes in antenna dimensions.

5.6 Conclusions

A modified loop antenna is integrated with EBGs. The structure is very compact. It shows good VSWR and directivity. The VSWR bandwidth is sufficient for covering four mobile frequency bands. The radiation in backward direction is also significantly reduced. This structure is a very suitable candidate for applications in telephone handsets.

6. Conclusions and Future Work

6.1 Conclusions

The main objective of this thesis was to explore design of novel antennas for possible applications in wireless communications. To achieve the objective suitable numerical methods were used for modeling, and limited measurements were performed. Two antennas were investigated, namely a compact, planar antenna with and without EBGs, and a wire antenna placed over an EBG Surface. The main contributions of the thesis are:

- A novel microstrip antenna was designed, optimized by using MoM simulations and measured. The antenna has a wide impedance bandwidth and is more compact compared to other broadband antennas. Equations for initial design were, developed and the mechanism of antenna operation was explored. The antenna performance (radiation patterns, gain, VSWR) was investigated. While the antenna has an excellent bandwidth (over 90 %), it has some shortcomings, namely the gain decreases at higher frequencies and antenna polarization varies with frequency. To show the generality of the idea two other antennas were designed on different substrates and for different frequency bands. To improve the gain at higher frequencies, the antenna was integrated with EBGs. Prototypes of the antennas were fabricated and measurements showed an excellent agreement with simulation results for the VSWR. Possible applications of this antenna are for laptop computers, PDAs and other wireless communication devices, which operate, in multi-path environment and for which the change in the radiation polarization would not be a problem.

- A wideband loop antenna was integrated with EBGs. The FDTD code was used to model the antenna and EBGs, after their initial design using simplified analytical approaches. This antenna was aimed specifically for the use on mobile handsets. Significant improvements in the VSWR and gain were obtained compared to

those for the same antenna without EBG and placed on the top of the handset box. The front to back ratio of the planar antenna structure was also good, suggesting that the power deposition in the user's head would be also lowered.

6.2 Future Work

Further investigations aimed at improvements and more complete characterization of both antennas could be undertaken. It is not possible to maintain the very broadband matching of the planar microstrip antenna and at the same time to have only one direction of the beam. On the other hand, the understanding the antenna performance that was achieved can lead to designs that have linear polarization in the same direction within narrower (but still sufficient) frequency range. Finally, for a given application the antenna needs to be evaluated in the environment in which it operates, e.g. on a PDA it may be close to the human body.

References

[1] Fujimoto, K., Henderson, A., Hirasawa, K., James, J.R., Small Antennas, Research Studies Press, UK, distributed by Wiley, USA 1987.

[2] Li, R.L., Tentzeris, E.M., Laskar, J., Fusco, V.F., Cahill, R., "Broadband loop antenna for DCS-1800/IMT-2000 mobile phone handsets", *Microwave and Wireless Components Lett.*, 12(8): 305-307, 2002.

[3] Schaubert, D. H., "A review of some microstrip antenna characteristics", *Microstrip Antennas* edited by D. M. Pozar and D. H. Schaubert, New York: IEEE Press, pp. 59-67, 1995.

[4] Bahl, I. J., P. Bhartia, *Microstrip Antennas,* Dedhuam, Massachusetts, Artech-House, 1980.

[5] Waterhouse, R. B., *Microstrip Patch Antennas - A Designer's Guide*, Kluwer Academic Publishers, 2003.

[6] Hall, P. S., "Probe compensation in thick microstrip patches", *Electron. Lett.*, 23(11): 606-607, 1987.

[7] Huynh, T., Lee, K. F., "Single layer single patch wide band microstrip antenna", *Electron. Lett.*, 31(16):1310-1312, 1995.

[8] Lee, K. F., Luk, K. M., Tong, K. F., Shum, S. M., Huynh, T., Lee, R.Q., "Experimental and simulation studies of coaxially fed U-slot rectangular patch antenna", *IEE. Proc. Microwave Antennas and Propag.*, 144(5): 354-358, 1997.

[9] Bhalla, R., Shafai, L., "Resonance behavior of single U-slot microstrip patch antenna", *Microwave Opt. Technol. Lett.*, 32(5):333-335, 2002.

[10] Luk, K. M., C. L. Mak, Y. L. Chow, K. F. Lee, "Broadband microstrip patch antenna", *Electron. Lett.,* 32(5):1442-1443, 1998.

[11] Muk, C. L., K. M. Luk, K. F. Lee, Y. L. Chow, "Experimental study of microstrip patch antenna with an L-shaped probe", *IEEE Trans. Antennas and Propag.,* 48:777-782, 2000.

[12] Paschen, D.A., "Practical example of integarted broadband matching of microstrip antenna elements", *Proceedings of the 1986 Antenna Applications Symp.*: 199-217, 1986.

[13] Sze, J-Yi, Wong, K-L, "Designs of broadband microstrip antennas with embedded slots", *APS 1999 Proceedings*, 2:936-939.

[14] Yang, F., Zhang, X-X, Ye, X., and Samii, Y.R., "Wide-band E-shaped patch antennas for wireless communications", *IEEE Trans. Antennas and Propag.,* 49(7):1094-1100, 2001.

[15] Targonski, S. D., Waterhouse, R. B., Pozar, D. M., " Design of wide-band aperture-stacked patch microstrip antennas", *IEEE Trans. Antennas and Propag.*, 46(9):1245-1251, 1998.

[16] Pozar, D. M., " A review of bandwidth enhancement techniques for microstrip antennas", *Microstrip Antennas* edited by D. M. Pozar and D. H. Schaubert, New York: IEEE Press, pp.157-166, 1995.

[17] Qin, Y., Gao, S., Sambell, A., Korolkiewicz, E., " Broadband patch antenna with ring slot coupling", *Electron Lett.*, 40(1):5-6, 2004.

[18] Fortino, N., Kossiavas, G., Dauvignac, J. Y., Staraj, R., "Novel antennas for ultrawideband communications", *Microwave Opt. Technol. Lett.*, 41(3):166-169, 2004.

[19] Parkar, G. S., Antar, Y. M. M., Ittipiboon, A., and Petosa, A., "Dual polarized microstrip ring antenna with good isolation", *Electron., Lett.,* 34(11):1043-1044, 1998.

[20] Kim, Y., Yun, W., Yoon, Y., "Dual-frequency and dual-polarization wideband microstrip antenna", *Electron. Lett.,* 35(17): 1399-1400, 1999.

[21] Yong, K., "Broad-band dual-polarized patch antennas fed by capacitively coupled feed and slot-coupled feed", *IEEE Trans. Antennas and Propag.,* 50(3):347-351, 2002.

[22] Yamazaki, M., Rahardjo, E.T., Hanneishi, M., "Construction of a slot-coupled planar antenna for dual polarization", *Electron. Lett.*, 30(22):1814-1815, 1994.

[23] Rahman, M., Stuchly, M. A., "Dual-polarization broadband patch antenna", *Microwave Opt. Technol. Lett.,* 22(6): 414-420, 1999.

[24] Yeh, S-H., Wong, K-L., Chiou, T-W, Fang, S-T., "Dual-band planar inverted F antenna for GSM/DCS mobile phones", *IEEE Trans. Antennas and Propag.*, 51(5):1124-1126, 2003.

[25] Lu, J-H, "Bandwidth enhancement design of single-layer slotted circular microstrip antennas", *IEEE Trans. Antennas and Propag.,* 51(5):1126-1129, 2003.

[26] Lu, J-H, "Broadband dual-frequency operation of circular patch antennas and arrays with a pair of L-shaped slots", *IEEE Trans. Antennas and Propag.,* 51(5):1018-1023, 2003.

[27] Liu, T. H., Zhang, W.X., "A novel single-layer patch antenna for GSM/DCS dual-band operation", *Microwave and Optical Tech. Lett.*, 38(3):195-198, 2003.

[28] Ooi, B.L., Lee, C.L, "A wideband meander-line probe-fed patch antenna", *Microwave Opt. Technol. Lett.*, 37(6):401-403, 2003.

[29] Sievenpiper, D.F., Romulo, L. Z., Broas, R. F. J., Alexopolous, N. G., Yablonovitch, E., "High impedance electromagnetic surfaces with a forbidden frequency band", *IEEE Microwave Theory and Tech.*, 47(11):2059-2074, 1999.

[30] Yang, F., Ma, K-P., Qian, Y., Itoh, T., "A uniplanar compact photonic-bandgap (UC-PBG) structure and its applications for microwave circuits", *IEEE Trans. Microwave Theory and Tech.*, 47(8):1509-1514, 1999.

[31] Caloz, C., Chang, C-C., Qian, Y., Itoh, T., "A novel multilayer photonic band-gap (PBG) structure for microstrip circuits and antennas", *APS 2001 Proceedings*, 2:502-505.

[32] Barley, A. S., Samii, Y. R., "Characterization of electromagnetic band-gaps composed of multiple periodic tripods with interconnecting vias: concept, analysis and design", *IEEE Trans. Antennas and Propag.*, 49(3):343-353, 2001.

[33] Gonzalo, R., Martinez, B., Maagt, P., Sorolla, M., "Improved patch antenna performance by using photonic bandgap substrates", *Microwave Opt. Technol. Lett.*, 24(4):213-315, 2000.

[34] Horii, Y., Tsutsumi, M., "Harmonic control by photonic bandgap on microstrip patch antenna", *IEEE Microwave Guided Wave Lett.*, 9(1):13-15, 1999.

[35] Gonzalo, R., Ederra, I., Mann, C., Maagt, P.de., " Radiation properties of terahertz dipole antenna mounted on photonic crystal", *Electron. Lett.*, 37(10): 613-614, 2001.

[36] Liu, T. H., Zhang, W. X., Zhang, M., "A spiral antenna backed on photonic bandgap material", *ISAP 2000 Proceedings*, 1:21–25.

[37] Yang, F., Samii, Y.R., "A low profile circularly polarized curl antenna over an electromagnetic bandgap (EBG) surface", *Microwave Opt. Tech. Lett.*, 31(4):264–267, 2001.

[38] Rahman, M., Stuchly, M. A., "Circularly polarized patch antenna with periodic structure", *IEE Proc. Microwave Antennas and Propag.*, 149(3):141-146, 2002.

[39] Brown, E. R., Parker, C. D., Yablonovith, E., "Radiation properties of a planar antenna on a photonic-crystal substrate", *J. Optic Soc. Amer. B, Opt. Phys.*, 10(2):404–407, 1993.

[40] Thevenot, M., Reineix, A., Jecko, B., "A dielectric photonic parabolic reflector", *Microwave Opt. Technol. Lett.*, 21(6):411–414, 1999.

[41] Broas, R. F. J., Sievenpiper, D. F., Yablonovitch, E., "A high impedance ground plane applied to a cellphone handset geometry", *IEEE Trans. Microwave Theory and Tech.*, 49(7):1262-1265, 2001.

[42] Hurtado, R., Klimczak, W., McKinzie, W. E., Humen, A., "Artificial magnetic conductor technology reduces weight and size for precision GPS antennas", presented at the Navigational National Technical Meeting, San Diego, CA, Jan 28–30, 2002.

[43] Cheype, C., Serier, C., Thevenot, M., Monediere, T., Reineix, A., Jecko, B., "An electromagnetic bandgap resonator antenna", *IEEE Trans. Antennas and Propag.*, 50(9):1285–1290, 2002.

[44] Botton, R. C. Jr., Computational Methods for Electromagnetics and Microwaves, John Wiley & Sons, Inc., 1992.

[45] Araki. K., Itoh, T., "Hankel transform domain analysis of open circular microstrip radiating structures", *IEEE Trans. Antennas and Propag.*, 25(1):84-89, 1981.

[46] Zurcher, J-F., Gardiol, F. E., Broadband Patch Antennas, Artech House Publications, 1995.

[47] Swanson, D. G., Hoefer, W. J. R., "Microwave circuit modeling using electromagnetic field simulation", Artech House Publications, 2003.

[48] Hubing, T. H., "Calculating the currents induced on wires attached to opposite sides of a thin plate", *ACES Collection of Canonical Problems*, pp. 9-13, 1990.

[49] Yee, K.S., "Numerical solution of initial boundary value problems involving Maxwell's equations in isotropic media", *IEEE Trans. Antennas and Propag., 14(5):*302-307, 1966.

[50] Taflove, A., Brodwin, M. E., "Numerical solution of steady-state electromagnetic scattering problems using the time-dependent Maxwell's equations", *IEEE Trans. Microwave Theory and Tech.,* 23(8):623-630, 1975.

[51] Taflove, A., Computational Electromagnetics: The Finite Difference Time Domain Method, Artech House Publications, 1995.

[52] Berenger, J.P., "A perfectly matched layer for the absorption of electromagnetic waves", *J. Comp. Phys.*, 114:185-200, 1994.

[53] Taflove, A., Brodwin, M.E., " Numerical solution of steady-state electromagnetic scattering problems using the time-dependent Maxwell's equations", *IEEE Trans. Microwave Theory and Techn.*, 23(8):623-630, 1975.

[54] Tirkas, P. A., Balanis, C. A., "Finite-difference time-domain method for antenna radiation", *IEEE Trans. Antennas and Propag.,* 40(3):334-340, 1992.

[55] Maloney, J. G., Shlager, K. L., Smith, G. S., "A simple FDTD model for transient excitation of antennas by transmission lines", *IEEE Trans. Antennas and Propag.*, 42(2):289-292, 1994.

[56] Chabolu, S., Mitra, R., "The analysis of microwave antennas using the FDTD method", *Microwave Journal,* 39(1):134-150, 1996.

[57] Help file of Ansoft Designer, Ansoft Corporation.

[58] Rambabu, K., Alam, M., Bornemann, J., Stuchly, M. A., "Compact wideband dual-polarized microstrip patch antenna", *APS-2004 Proceedings.*

[59] Gupta, K. C., Garg, R., Bahl, I., Bhartia, P., Microstrip Lines and Slotlines, Artech House Publications, 1996.

[60] Katsibas, K. D., Balanis, A., Tirkas, P. A., Birtcher, C. R., "Folded loop antenna for mobile hand-held units", *IEEE Trans. Antennas and Propag.,* 46(2):260-266, 1998.

[61] Yang, F., Samii, Y. R., "Reflection phase characterizations of the EBG ground plane for low profile wire antenna applications", *IEEE Trans. Antennas and Propag.,*51(10): 2691-2703, 2003.

[62] Rahman, M., "Modeling of compact antennas for wireless communication in complex environment", Ph.D. Thesis, University of Victoria, 2001.

[63] Balanis, C. A., Antenna Theory Analysis and Design, Harper and Row Publishers, NY, 1982.

[64] Tong, K. F. , Luk, K. M., Lee, K. F., Shum, S. M., " Analysis of Broadband U-slot Microstrip Antenna", *APS 1997 Proceedings*, 1: 110-113.

[65] Pozar, D. M. , Duffy, S., Herscovici, N., "A comparison of commercial software packages for microstrip antenna analysis", *APS 2000 Proceedings,* 1(1):152-155.

Appendix A Antenna Parameters

Since this research is concerned with designing and modeling antennas, some basic antenna parameters such as radiation pattern, input impedance, gain, directivity and polarization are described. These parameters are important for the characterization of an antenna. All these definitions are from [63] unless otherwise indicated. The definitions inside quotation marks are from IEEE Standard Definitions of Terms for Antennas (IEEE Std 145-1973).

A.1 Radiation Pattern

The radiation pattern of an antenna is defined as the "graphical representation of the radiation properties of the antenna as a function of angular coordinates. In most cases the radiation pattern is determined in the far field region and is represented as a function of angular coordinates. Radiation properties include radiation intensity, field strength, phase or polarization."

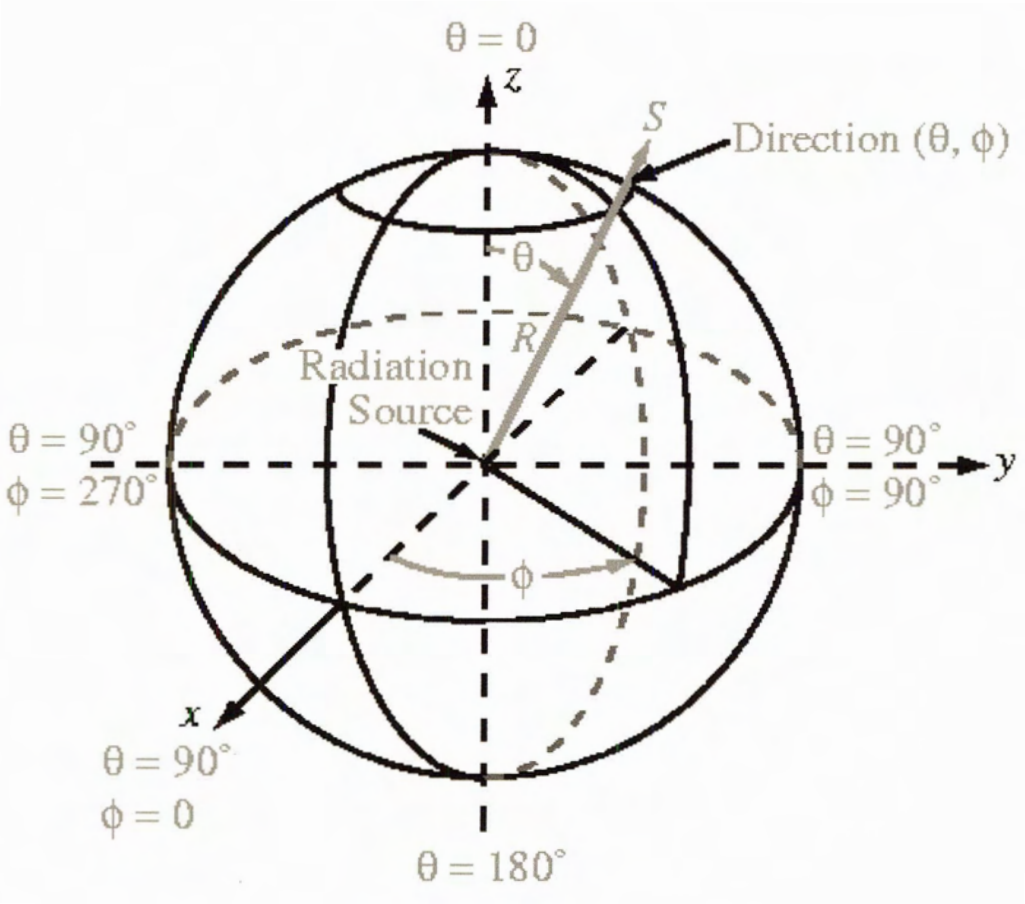

Figure A. 1 Spherical coordinate system

Radiation pattern of an antenna can be either a power pattern or a field pattern. Referring to Figure A.1, a two dimensional pattern is obtained by fixing one of the angle (θ or ϕ) while varying the other. Keeping ϕ constant, and varying θ ($0° \leq \theta \leq 180°$) gives elevation pattern. Similarly, keeping θ constant, and varying ϕ ($0° \leq \phi \leq 360°$) gives azimuthal pattern.

The performance of an antenna is often described with the help of patterns in two principal planes, which are called E-plane and H-plane. The E-plane for a linearly polarized antenna is defined as "the plane containing the electric field vector and the direction of maximum radiation". The H-plane is defined as "the plane containing the magnetic field vector and the direction of maximum radiation". Radiation pattern can be broadly classified as isotropic, directional and omnidirectional. An isotropic radiator is

defined as "a hypothetical antenna having equal radiation in all directions". A directional antenna is one "having the property of radiating or receiving electromagnetic waves more effectively in some directions than in others." An omnidirectional pattern is defined as one "having essentially nondirectional pattern in any orthogonal plane".

A.2 Input impedance and VSWR

Input impedance is defined as "the impedance presented by an antenna at its terminals or the ratio of the voltage to current at a pair of terminals or the ratio of appropriate components of the electric to magnetic fields at a point".

The VSWR of an antenna is defined as the ratio of the reflected and incident voltage waves at the input terminals of the antenna and can be expressed as

$$VSWR = \frac{|Z_{in} + Z_0| + |Z_{in} - Z_0|}{|Z_{in} + Z_0| - |Z_{in} - Z_0|} \qquad \text{(A.1)}$$

Here Z_0 is the characteristic impedance of the feeding transmission line and Z_{in} is the input impedance of the antenna.

A.3 Bandwidth

The bandwidth of an antenna can be defined as the range of frequencies over which the performance of the antenna, with respect to some characteristics, conforms to a specified standard. Bandwidth can be defined in one of several ways. [Schaubert]

1) **Impedance Bandwidth:** The impedance variation with frequency of the antenna results in a limitation of the frequency range over, which the antenna can be matched to a feed line. Impedance bandwidth is usually specified in terms of a return loss (typically less than -10 dB) or maximum VSWR (typically less than 2) over a frequency range.

2) **Pattern Bandwidth:** The beam width, side lobe levels and gain of an antenna all vary with frequency. If any of these quantities is specified as a minimum or maximum, finding pattern bandwidth is necessary.

3) **Polarization or Axial Ratio Bandwidth:** The polarization properties (linear or circular) of an antenna typicaly should remain constant within the operating frequency range. Specifying a maximum cross polarization level for linear polarization or axial ratio for the circular polarization can be used to find this bandwidth. Polarization loss factor is also often used to characterize antenna polarization.

A.4 Directivity, Efficiency and Gain

The directivity of an antenna is defined as "the ratio of the radiation intensity in a given direction from the antenna to the radiation intensity averaged over all directions. The average radiation intensity is equal to the power radiated by the antenna divided by 4π. If the direction is not specified, the direction of maximum radiation is implied." Directivity is defined as:

$$D = \frac{U}{U_0} = \frac{4\pi U_{\max}}{P_{rad}}$$

$$D_{\max} = D_0 = \frac{U_{\max}}{U_0} = \frac{4\pi U_{\max}}{P_{rad}} \qquad \text{(A.2)}$$

where:

D =directivity (dimensionless)
D_0 =maximum directivity (dimensionless)
U =radiation intensity (Watts/unit solid angle)
U_{max} =maximum radiation intensity (Watts/unit solid angle)
U_0 =radiation intensity of isotropic radiator (Watts/unit solid angle)
P_{rad} =total radiated power (Watt)

A more important measure of antenna performance is antenna gain. The gain of an antenna is defined as "the ratio of the radiation intensity, in a given direction, to the radiation intensity that would be obtained if the power accepted by the antenna were radiated isotropically. The radiation intensity corresponding to the isotropical radiated power is equal to the power accepted (input) by the antenna divided by 4π."

Antenna efficiency accounts for the losses at the input terminals and within the structure of the antenna. Losses may occur due to the mismatch between the feeding line and the antenna, and also due to conductor and dielectric losses.

The overall efficiency can be expressed as $e_t = e_r e_{cd}$ where e_t is the over all efficiency, e_r is the reflection efficiency and e_{cd} is the conduction and dielectric efficiency. The reflection efficiency is $(1-|\Gamma|^2)$ where Γ is the reflection coefficient and $e_{cd} = \frac{R_r}{R_r + R_L}$ where R_r an R_L are radiation and loss resistance respectively.

A.5 Polarization

Polarization of an antenna is defined as "the polarization of the wave transmitted (radiated) by the antenna." The polarization of a radiated wave is defined as "the property of a radiated wave describing the time varying direction and relative magnitude of the electric field vector; specifically, the figures traced as a function of time by the extremity of a vector at a fixed location in space and the sense in which it is traced, as observed along the direction of propagation".

Polarization can be classified as linear, circular and elliptical.

Linear polarization: A time harmonic field is linearly polarized at a given point in space if the electric (or magnetic) field vector is always oriented along the same straight line at

every instant of time. This can happen if the field vector possesses (a) only one component or (b) two orthogonal components that are in time phase or 180° out of phase.

Circular polarization: Circular polarization can be obtained only when the magnitude of the two orthogonal field components have same magnitude and the phase difference between them is an odd multiple of 90°.

Elliptical polarization: Elliptical polarization can be achieved when there are two orthogonal field components and (a) they are not equal and their phase difference is an odd multiple of 90° or (b) when the phase difference is not an odd multiple of 90° irrespective of their magnitude.

Appendix B Modeling of Selected Antennas

To verify that the available software packages are capable of reliable modeling of antennas of similar geometries to the novel antenna under development, modeling results were compared with published measurements for selected antennas previously described in literature. The following antennas were considered for the comparison:

a) U-slot antenna from [64], and
b) E shaped antenna from [14]

Additionally, performance for a planar antenna previously developed at University of Victoria was evaluated. Comparison was made between the results from different codes, since measurement data were not available.

Figure B.1 and Table B.1 show the comparison of VSWR obtained from different codes and measurements for the U slot antenna.

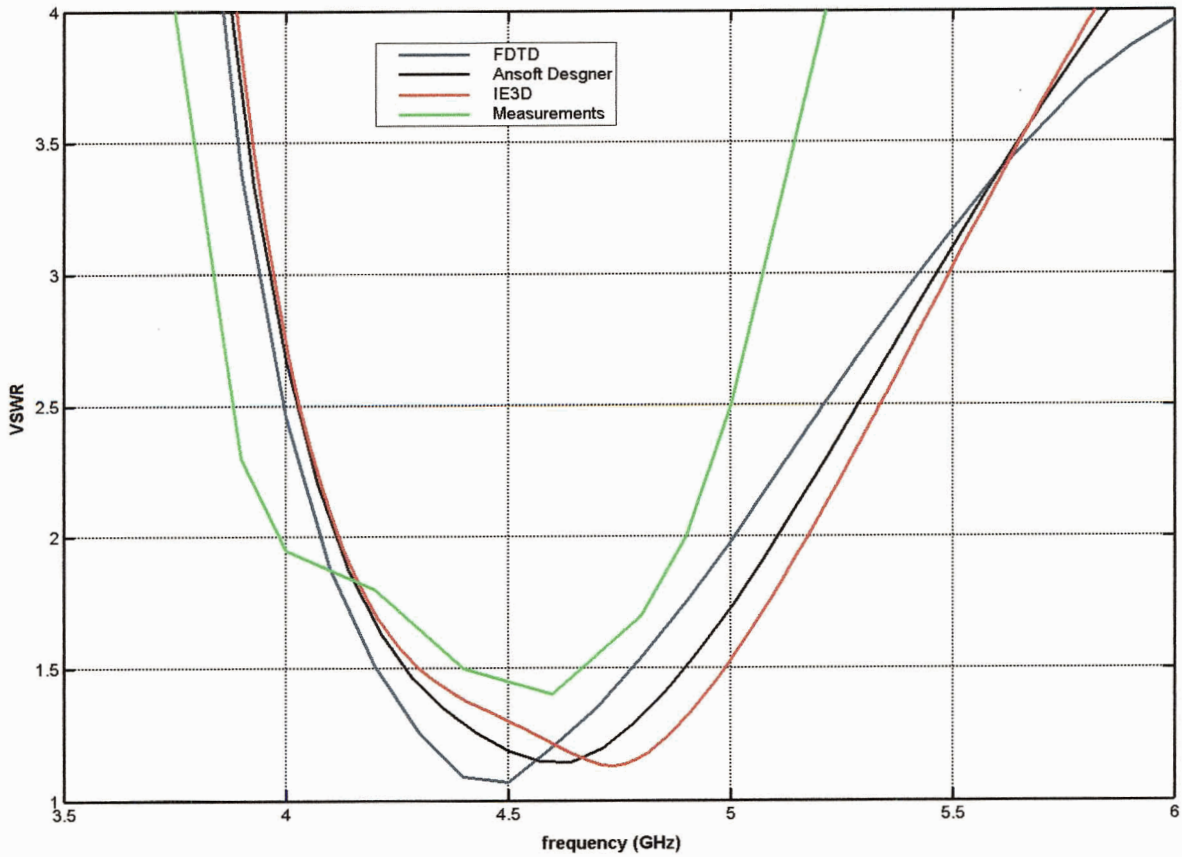

Figure B. 1 Comparison of VSWR obtained from simulations and measurements for the U-slot antenna

Table B. 1 Comparison of simulation results and measurements for U-slot antenna

	VSWR <2 Bandwidth
Measurements	20.96 % (3.97 - 4.9 GHz)
FDTD	20.5 % (4.07 - 5 GHz)
IE3D	21.28 % (4.2 - 5.2 GHz)
Ansoft Designer	25.53 % (4.1 - 5.3 GHz)

All the packages give similar results for this antenna.

The results for the E shaped antenna are shown in Figure B.2 and Table B.2.

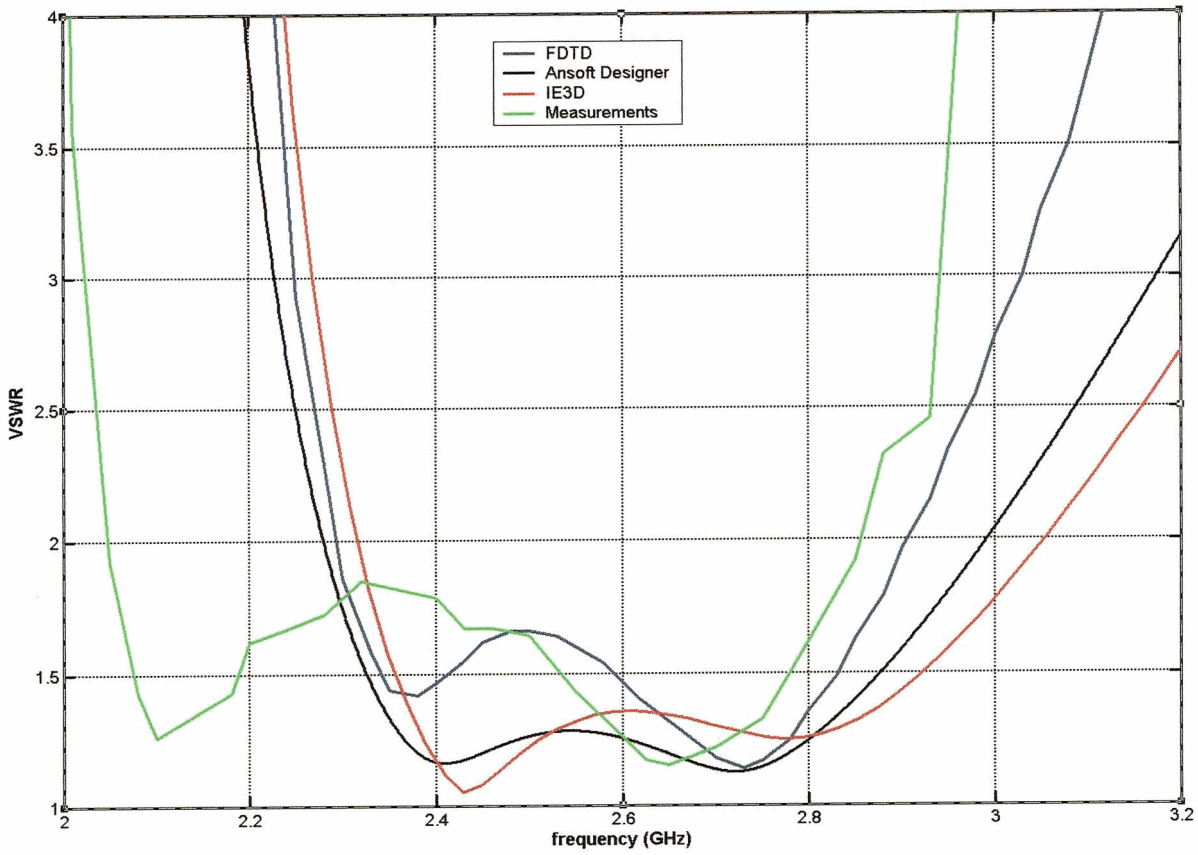

Figure B. 2 Comparison of VSWR obtained from simulations and measurements for the E shaped antenna

Table B. 2 Comparison of simulation results and measurements for E shaped antenna

	VSWR < 2 Bandwidth
Measurements	32.6 % (2.05 - 2.85 GHz)
FDTD	22.93 % (2.34 - 2.93 GHz)
IE3D	27.19 % (2.32 – 3.05 GHz)
Ansoft Designer	27.12 % (2.28 – 2.99 GHz)

The results for the planar antenna planar antenna developed at University of Victoria are shown in Figure B.3 and Table B.3.

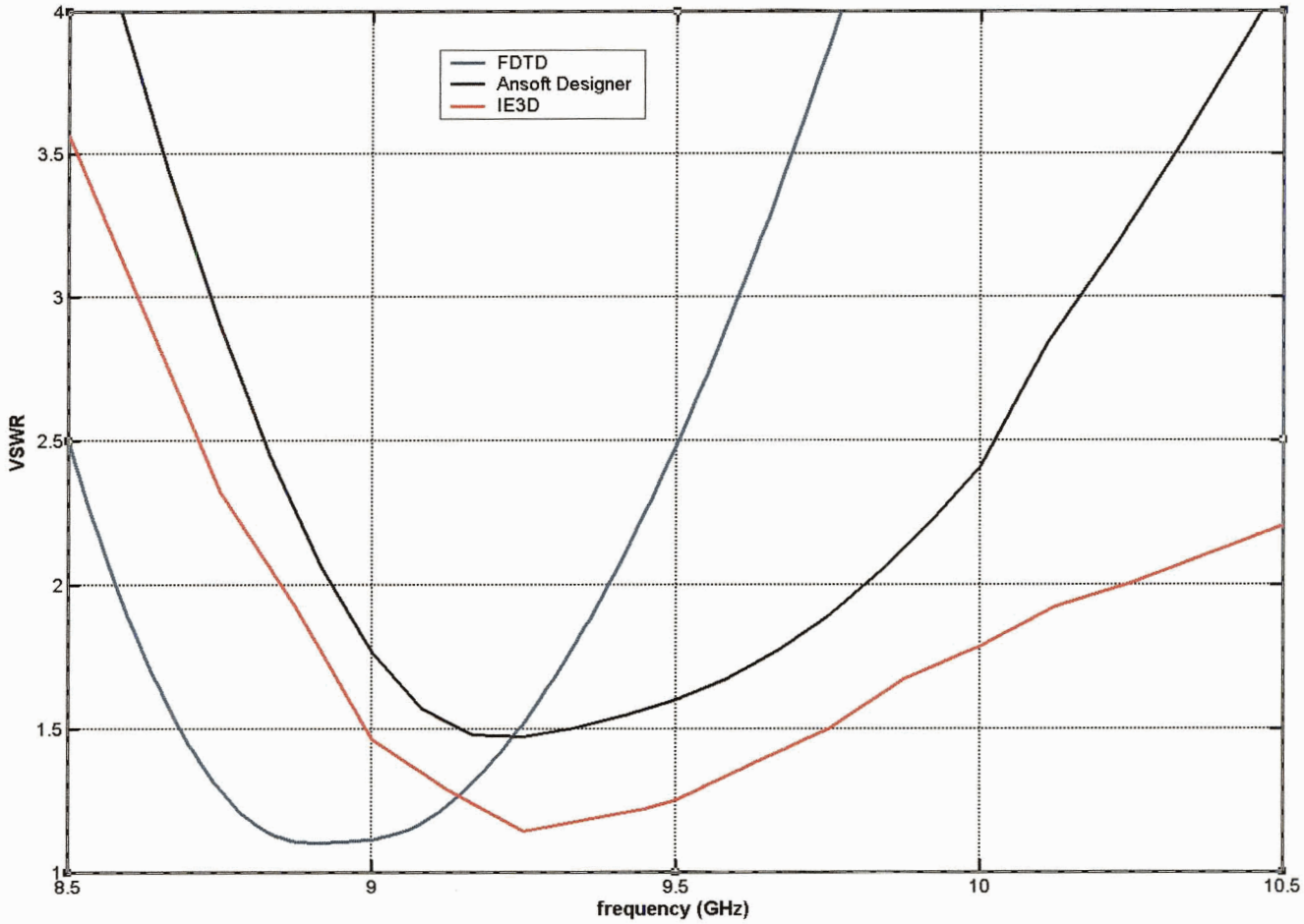

Figure B. 3 Comparison of VSWR obtained from simulation for planar antenna

Table B. 3 Comparison of simulation results for planar antenna developed in University of Victoria

	VSWR < 2 Bandwidth
FDTD	9.41 % (8.6 - 9.45 GHz)
IE3D	14.43% (8.87 - 10.25 GHz)
Ansoft Designer	9.4% (8.92 - 9.8 GHz)

For this structure, IE3D gives significantly different result than the other two packages.

From the above results, it can be seen that all these packages give reasonably good results for different antenna structures. However, their accuracy is dependent on the structure being analyzed [65]. For the U shaped antenna, the three codes give similar results that are also in relatively good agreement with measurements. For the E-shaped antenna, again all codes give similar results. However in this case the measurements indicate a wider frequency range where the antenna is impedance matched. The greatest differences in modeling results are for the planar antenna. The bandwidth given by IE3D is over 50% wider than that shown by the two other codes. Considering the three antennas, it can also be noted that IE3D shifts the operating band towards higher frequencies.

In summary, from these preliminary tests of the software packages, all of them appear to perform reasonably. More specifically, it is difficult from these data to decide which of the two MoM based codes is better. Both of them require less computational resources and less effort from the researcher than the FDTD code (which does not have a GUI).

Appendix C Measurement Results

Results of VSWR measurements not mentioned else where in the thesis are presented here. All measurements were done using network analyzer HP 8720 C. Results for three cases are presented here.

Case 1: one EBG layer placed 3.5 mm away from the antenna
Case 2: two EBG layers placed 3.5 mm away from the antenna
Case 3: three EBG layers placed 5.5 mm away from the antenna

Figure C.1 shows the results for a single layer of EBG placed 3.5 mm away from the antenna.

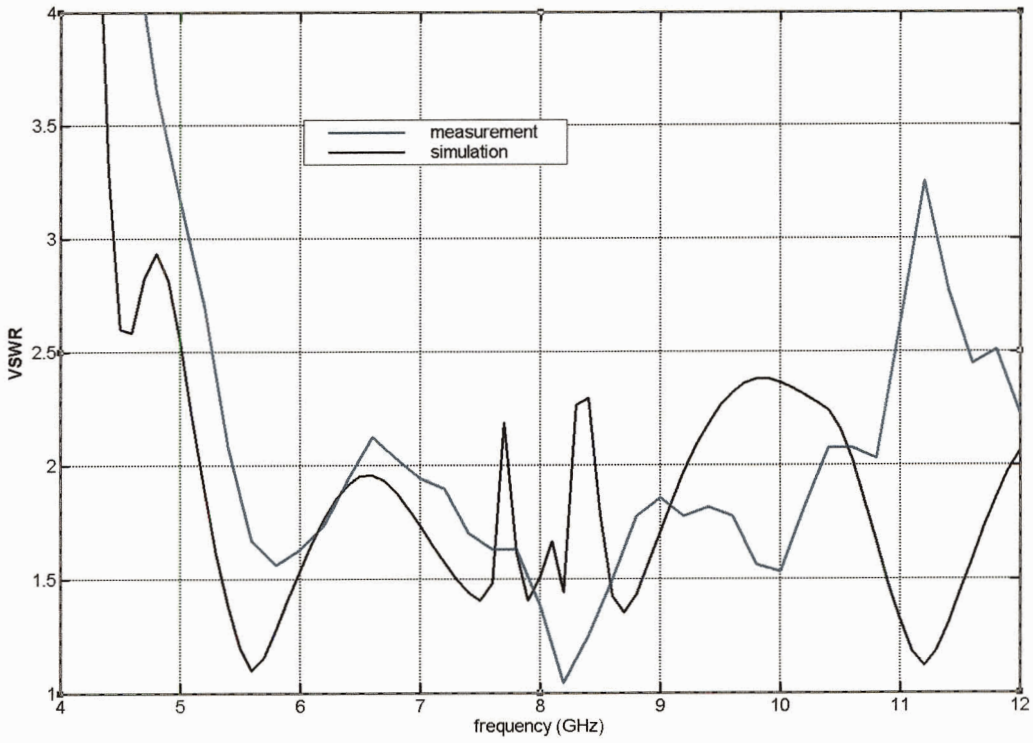

Figure C. 1 VSWR for antenna with single EBG layer 3.5 mm away from antenna (VSWR < 2.2 for 5.35 - 10.8 GHz)

Figure C.2 presents the results for two layers of EBG placed 3.5 mm away from the antenna. The antenna acts as a dual band antenna for this case.

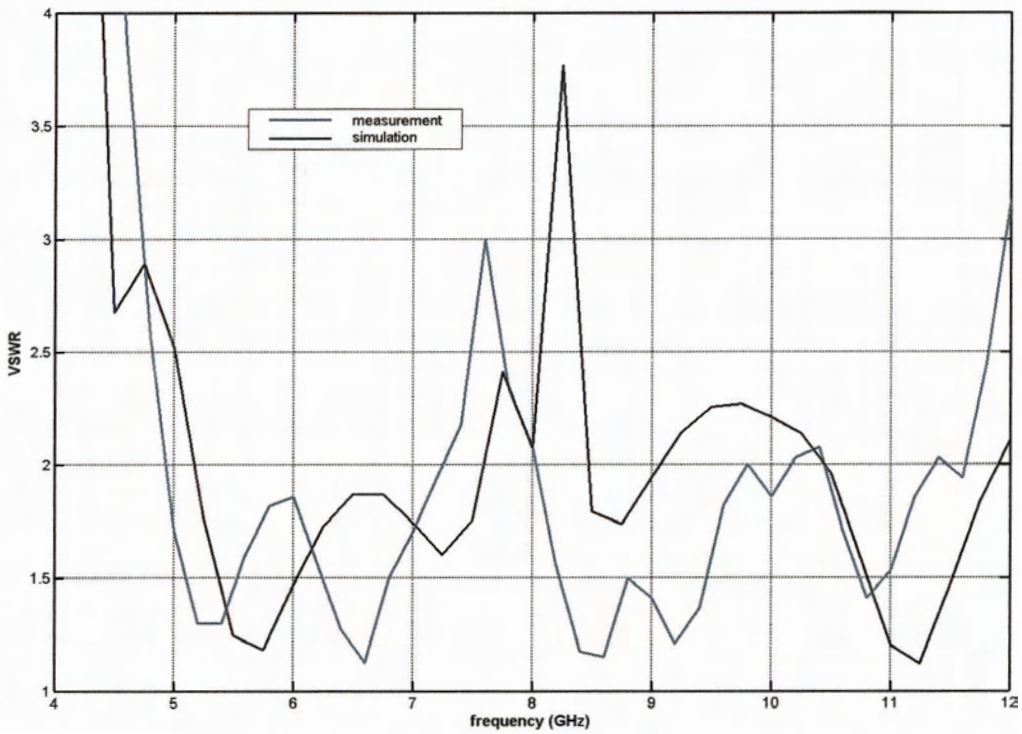

Figure C. 2 VSWR for antenna with two EBG layers 3.5 mm away from antenna (VSWR < 2.2 for 4.9 – 7.4 GHz and 7.9 – 11.7 GHz)

Figure C.3 shows the results for three layers of EBG placed 5.5 mm away from the antenna.

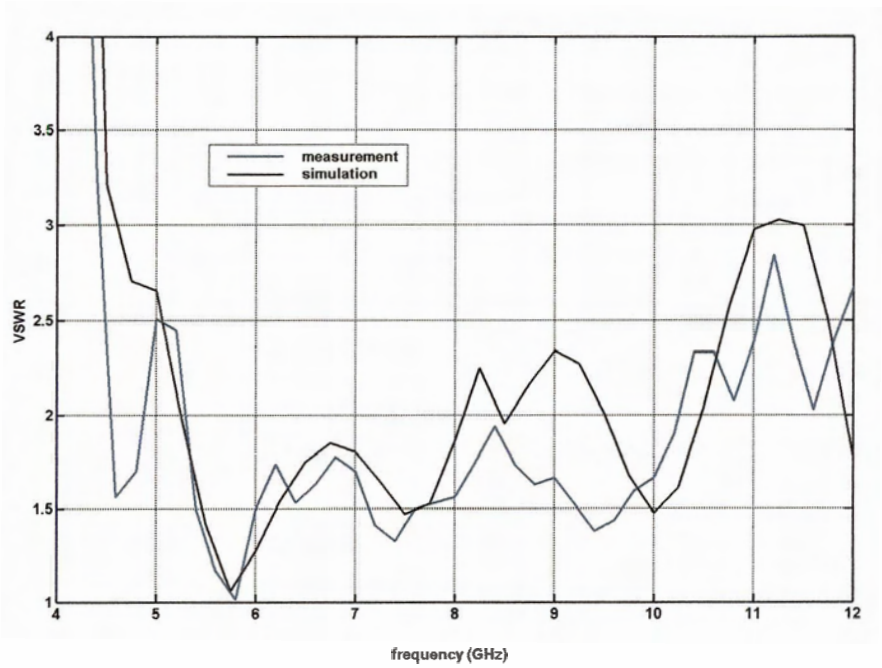

Figure C. 3 VSWR for antenna with three EBG layers 5.5 mm away from antenna (VSWR < 2.2 for 5.25 – 10.9 GHz)

The results from measurements and simulations are summarized in Table C.1.

Table C. 1 Summary of measured and simulation results for antenna with EBGs

No of EBG layer	Distance from antenna (mm)	VSWR ≤ 2.2 Bandwidth (measured)	VSWR ≤ 2.2 Bandwidth (simulated)
One	3.5	67.5% (5.35 – 10.8 GHz)	59.8% (5.1 – 9.45 GHz)
Two	3.5	50.5 % (4.9 – 7.4 GHz) 38.8 % (7.9 – 11.7 GHz)	44.9 % (5.1 – 8.05 GHz) 43.3 % (8.5 – 13.2 GHz)
Three	5.5	69.9 % (5. 25 – 10.9 GHz)	68.4 % (5.2 – 10.6 GHz)

For all three cases, results from simulations are in reasonably close agreement with those from measurements. The difference between them at some frequencies is probably due to misalignment of the two layers of the antenna.